Design and Application of a Plasma Impedance Monitor for RF Plasma Diagnostics

A thesis for the degree of M.Sc.

Presented to

DUBLIN CITY UNIVERSITY

By

KIERAN DOBBYN B.Sc.,

Plasma Research Laboratory

School of Physical Sciences

DUBLIN CITY UNIVERSITY

June 2000

Research Supervisor: Dr. Michael B. Hopkins

Internal Examiner: Dr. David Vender

External Examiner: Prof. Norman Brown,

University of Ulster at Coleraine

DECLARATION

I hereby certify that this material, which I now submit for assessment on the programme of study leading to the award of M.Sc., is entirely my own work and has not been taken from the work of others save and to the extent that such work has been cited and acknowledged within the text of my work.

Signed: Kieran Dobbyn
Kieran Dobbyn

Student ID: 95971629

Date: 18th September 2000

ACKNOWLEDGEMENTS

The *Plasma Impedance Monitor (PIM)* is the result of a commercial project funded by *Scientific Systems Ltd* and is now a leading product for *Scientific Systems Ltd* under the trade name *SmartPIM* *Scientific Systems Ltd* designs and manufactures RF plasma sensors and instruments for RF plasma process control and diagnostics

Due to the complexity and commercial nature of the project it was necessary to employ the skills of other people to help with the design of the PIM in order to complete the project within the period required by *Scientific Systems Ltd* I wish, therefore, to acknowledge those people who have helped to successfully complete the design of the PIM

The main project tasks, and those responsible, can be outlined as follows

Project Concept

The concept and basic design of a Plasma Impedance Monitor came from Dr Mike Hopkins (*Plasma Research Laboratory, DCU*), who, through regular meetings with the key personnel, ensured that the project goal and system design were completed as required Mike was directly involved in all aspects of the system design, including both hardware and software

Project Management

It was the author's responsibility to ensure that the project schedule was maintained through regular meetings and correspondence with the personnel involved

RF Vector Integrator

Mr John Matthews (*Teltec Irl, DCU*) performed the majority of the digital electronics design and the final circuit board layout John was contracted by *Scientific Systems Ltd* to do some of design due to commercial constraints The author was involved in most of the analogue electronics design and in some of the digital electronics design The author was also responsible for component purchasing and the manufacture of the first prototypes The author has been responsible for all subsequent design modifications of the *RF Vector Integrator* resulting in the final system as traded by *Scientific Systems Ltd*

IV Sensor

Mr Ciaran O'Morain (*Scientific Systems Ltd*) designed the mechanical components of the IV Sensor The author was responsible for the design of the PCB sensor

PIMSoft.

Mr Andrew Graydon (*Scientific Systems Ltd*) performed the design of PIMSoft

PIMCode

The author performed the design of PIMCode, with help from Mike and Andrew with the communication and analysis sections

Testing

Mr John Matthews and the author performed functional tests of the various sections of the RF Vector Integrator Tests of the complete system (i e *RF Vector Integrator*, *IV Sensor* and software applications) were performed by those responsible for each component The author performed testing of the system using a test rig known as a Dynamic Dummy Load, or DDL

Calibration

The author performed calibration of the complete system

I would also like to thank and acknowledge everyone else who helped me during this period, especially my friends and companions in DCU, the technicians (especially Alan and Des), lecturers, and the other members of the Plasma Research Laboratory - Sam, Barry, Deirdre, Brendan, Jim, Seamus, the two Catherine's, Declan and John

A word of thanks to my colleagues in *Scientific Systems Ltd* for their help and assistance and for acquiring some of the application data used in this thesis

I would like to thank my family for their encouragement and for showing an interest in my work and also to Martina for her understanding and support, all of whom I'm sure still don't know what I am doing or what a plasma is

Finally, a special word of thanks to my parents without whose support during both my education and personal life I would not now be writing this It is with great sadness that I cannot share this moment with my Father (due to his bereavement) who has undoubtedly had the biggest influence on my life and career I therefore dedicate this dissertation to him

CONTENTS

DECLARATION I

ACKNOWLEDGEMENTS II

CONTENTS IV

ABSTRACT VI

CHAPTER 1 - INTRODUCTION TO PLASMA 1

1 1 PLASMA 1

1 2 PLASMA PARAMETERS 3
1 2 1 PLASMA DENSITY 3
1 2 2 DEBYE LENGTH 3
1 2 3 PLASMA SHEATHS 4
1 2 4 PLASMA IMPEDANCE AND RF HARMONICS 5

CHAPTER 2 - MATERIALS PROCESSING USING RF PLASMAS 7

2 1 PLASMA PROCESSING 7

2 2 PLASMA PROCESS REACTORS 10
2 2 1 CAPACITIVE RF PROCESS REACTORS 10
2 2 2 INDUCTIVE RF REACTORS 12

CHAPTER 3 - PLASMA IMPEDANCE MONITOR 14

3 1 PRESENT MEASUREMENT TECHNIQUES 15
3 1 1 CONVENTIONAL IV SENSOR 15
3 1 2 PIM IV SENSOR 17

3 2 WAVEFORM SAMPLING 19
3 2 1 COHERENT SAMPLING 19
3 2 2 SIGNAL AVERAGING 22

3 3 RF VECTOR INTEGRATOR CARD 23
3 3 1 PRINCIPLE OF OPERATION 24
3 3 2 SYSTEM SOFTWARE 26

CHAPTER 4 - PIM CALIBRATION 27

4 1 RF VECTOR INTEGRATOR CALIBRATION 28

4 2 IV SENSOR CALIBRATION 30

4 3 TESTING 32

CHAPTER 5 - PIM MEASUREMENT PERFORMANCE 35

5 1 VOLTAGE MEASUREMENT REPEATABILITY 37

5 2 CURRENT MEASUREMENT REPEATABILITY 40

5 3 PHASE MEASUREMENT REPEATABILITY 43

5 4 MEASUREMENT RESOLUTION 46

CHAPTER 6 - PLASMA DIAGNOSTICS AND PIM APPLICATIONS..........48

6 1 PLASMA DIAGNOSTICS 48

6 1 1 IMPEDANCE PROBES 49

6 2 PIM APPLICATIONS 51

6 2 1 RF POWER DELIVERY AND MATCH UNIT VARIATIONS 52

6 2 2 CHAMBER CLEAN END POINT 55

6 2 3 ETCH END POINT 56

6 3 OTHER POSSIBLE APPLICATIONS 57

CHAPTER 7 - CONCLUSION 58

APPENDIX A...59

REFERENCES 60

ABSTRACT

This thesis presents the design and application of a *Plasma Impedance Monitor* (PIM) as a plasma diagnostic for use with RF plasmas, focusing on its potential use in the semiconductor manufacturing industry The plasma impedance monitor system was designed to measure the amplitude and phase of the first five Fourier components (harmonics) of the plasma voltage and current of RF plasma process reactors

The first two chapters of this thesis discuss Plasma and Plasma Process Reactors as commonly used in the manufacture of semiconductors The most important parameters of a plasma in terms of materials processing are introduced as are the most common types of plasma process reactors and their characteristics

Chapters 3 and 4 discuss the PIM hardware and its method of calibration In chapter 3, the RF sensor and waveform sampling card, known as the IV Sensor and RF Vector Integrator respectively, are discussed in detail The technique of measuring the RF voltage and current using the IV Sensor and the unique waveform sampling technique used by the sampling card are explained In chapter 4, the method of calibration for the IV Sensor and RF Vector Integrator are explained Finally, the use of a Dynamic Dummy Load (DDL) to test the performance of the system is shown

Chapter 5 demonstrates the measurement repeatability and resolution of the PIM as used with a commercial plasma process reactor In chapter 6 some applications of the PIM for use in the semiconductor manufacturing industry are explained and demonstrated

As the manufacture of integrated circuits becomes more complex due to the reduction in component size, improved control of the manufacturing processes becomes essential Present day plasma processing tools provide real-time information such as RF power, chamber pressure, temperature, gas flow rate and gas composition that are used to control the process However, the reduction in device geometry, the need for higher yield, and the high cost of equipment ownership means that engineers require tighter control of the process and must be able to diagnose process and machine faults quickly and efficiently

Plasma-based processing systems can be characterised by their RF electrical parameters and it has been shown that changes in process conditions such as RF power or matching efficiency can be correlated to variability in process results and wafer quality The use of a plasma impedance monitor to measure and control the electrical properties of the RF discharge, and ultimately detect or predict process faults, can therefore become a most valuable process diagnostic

Chapter 1

INTRODUCTION TO PLASMA

Chemically reactive plasma discharges are widely used to modify the surface properties of materials It is due to this development that plasma processing has now become an essential process of some of the largest manufacturing industries in the world Most applications based on plasma enhanced chemical processing focus on treating solid surfaces, film deposition, modification of surfaces, and etching of surface layers [1,2,6]

1.1 Plasma

Plasma is the fourth state of matter [2] and is the state of most of the visible matter in the universe The solid, liquid, and gaseous states of matter that occur at the surface of the earth are not typical of matter in the universe at large In a plasma, the energy of the particles is so great that the electric forces that bind the electrons to the nucleus of the gas atoms are overcome The resulting assembly can be thought of as a gas consisting of positively and negatively charged particles moving in random directions, that is, on average, electrically neutral The motion of the charged particles can cause local concentrations of charges that affect the motion of other particles some distance away Therefore, the elements of the plasma can affect each other resulting in the plasma having a collective behaviour [1,2,3] It is due to this collective behaviour that plasma is referred to as the fourth state of matter

The majority of plasmas used for processing of materials are weakly ionised plasmas Weakly ionised plasmas are plasma having a very small percentage of charged particles in relation to neutral particles That is, the density of electrons, n_e, and ions, n_i, are only a small fraction of the density of the neutral particles, n_n Typically, the degree of ionisation is of the order of 10^{-4} with the result that the plasma is essentially a neutral ground state gas [3] However, it is the interaction, quantity and properties of the

various particles that determine the type of chemical process that a particular plasma will perform

A plasma is obtained when sufficient energy, higher than the ionisation energy, is added to atoms of a gas, causing ionisation and production of ions and electrons The plasma is usually sustained by providing electromagnetic energy to the gas in different forms such as direct current, radio frequency and microwaves, for example Plasmas are often referred to as gas discharges because the most common way to produce plasma is by passing an electrical current through the gas

A simple RF plasma discharge is shown schematically in Figure 1 1 It consists of a RF voltage source that drives current through a low-pressure gas between two parallel conducting plates or electrodes The atoms of the gas "'break down" or "decompose" into freely moving charged particles that form a weakly ionised plasma The plasma state is generated due to sufficient energy being supplied to the gas atoms from the external source that results in ionisation of the gas atoms

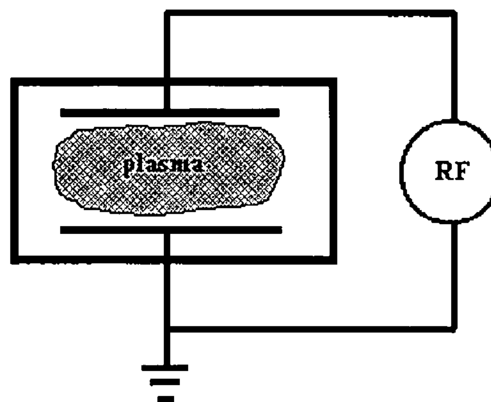

Fig 1 1 – Simple Plasma Discharge

1.2 Plasma Parameters

Plasma parameters are attributes of plasmas that allow a particular plasma to be described or compared to other similar plasmas These characteristics arise from the basic nature of the plasma in that it is a partially ionised gas with equal numbers of positive and negative charges

1 2 1 Plasma Density

The plasma density, that is the density of electrons, n_e, and ions, n_i, is an important parameter in plasma processing The efficiency of the processes occurring in the plasma and their reaction rates are generally dependent directly on the density of the charged particles [1] The electrons and ions affect the reactions occurring in plasma in different ways, but specifically, the reactions are controlled, or affected more by ion chemistry [2,8,13] It is therefore important to achieve high ion densities to increase the rates of reactions involving ions

1 2 2 Debye Length

In a plasma, electrons are attracted to the vicinity of an ion and shield its electrostatic field from the rest of the plasma Similarly, an electron at rest repels other electrons and attracts ions This effect alters the potential in the vicinity of a charged particle If a plasma had an excess of positive or negative particles, this excess would create an electric field and the electrons will move to cancel the charge The response of charged particles to reduce the effect of local electric fields is called *Debye Shielding* and the shielding gives the plasma its quasi-neutrality characteristic

The electric potential developed is mostly near the surface of the particle, extending over a distance λ_D, called the *Debye Length*, which is defined by [1,3]

$$\lambda_D = \left(\frac{\varepsilon_0 k T_e}{n_e e^2} \right)^{1/2} \qquad (1\ 1)$$

where
ε_0 = permittivity of free space
k = Boltzmann's constant
T_e = electron temperature
n_e = electron density
e = charge of the electron

As indicated by the above equation, the Debye length decreases with increasing electron density An ionised gas is considered a plasma only if the density of the charged particles is large enough such that λ_D<<L, where L is the dimension of the system [3]

1 2 3 Plasma Sheaths

When ions and electrons reach a surface that is in contact with the plasma, they recombine and are lost from the plasma Electrons have a much higher thermal velocity than ions and reach the surface faster, leaving the plasma with a positively charged region in the vicinity of the surface An electric field therefore develops near the surface in such a way as to make the net current zero As a result, the surface achieves a negative potential relative to the plasma or, in other words, the surface is at a negative self-bias relative to the plasma [3,4]

The plasma is therefore normally at a positive potential relative to any surface in contact with it The potential developed between the surface and the plasma bulk is confined to a layer of thickness of several Debye lengths This layer of positive space charge that exists around all surfaces in contact with a plasma is called the *Plasma Sheath* The sheath potential, V_s, is the electric potential developed across the plasma sheath Only electrons having sufficiently high thermal energy will penetrate the sheath and reach the surface, which, being negative relative to the plasma, tends to repel the electrons The value of the sheath potential adjusts itself in such a way that the flux of

these electrons is equal to the flux of ions reaching the surface Its value, for a planar surface, is given by [1]

$$V_s = \frac{kT_e}{2e}\ln\left(\frac{m_e}{2\,3m_i}\right) \qquad (1\,2)$$

where m_e = mass of electron
m_i = mass of ion

Sheaths form around any surface in contact with the plasma For example, a wafer will have a sheath formed around it The sheath potential will directly influence the energy with which the ions strike the wafer and the resulting kinetic energies can severely affect a growing film or etching process [1,3,8]

1 2 4 Plasma Impedance and RF Harmonics

Models of RF discharges have been proposed by various researchers, and have led to the development of equivalent circuit models of plasmas [45,46,47,52] By experiment, the electrical characteristics of plasmas can be determined and later verified using the plasma models For low-pressure RF discharges, a slab of plasma of width l and cross-sectional area A has an impedance that is inductive with a magnitude that is given by [2]

$$Z = \frac{1}{j\omega C} \qquad (1\,3)$$

with

$$C = \frac{\varepsilon_p A}{l} \qquad (1\,4)$$

where ε_p = plasma dielectric constant
A = cross-sectional area of plasma slab
l = width of plasma slab

However, the sheath regions are capacitive and, in many applications, they have a larger impedance than that of the bulk plasma such that almost all of the applied RF voltage appears across the sheaths rather than the bulk plasma

The width of the sheaths, and hence their impedance, vary with the applied RF current, generating harmonics of the RF voltage The capacitance of a sheath region can be expressed as [2,48,49,50]

$$C = \frac{\varepsilon_s A}{S(t)} \tag{1 5}$$

where ε_s = sheath dielectric constant
A = cross-sectional area of plasma slab
$S(t)$ = sheath thickness

Chapter 2

MATERIALS PROCESSING USING RF PLASMAS

The semiconductor manufacturing industry is the most important user of plasma-based processes The plasma process is used as a miniature chemical factory in which precursor gases are broken into positive ions and chemically reactive agents which then flow to and physically react at the surface of the substrate Plasma processes are used to deposit (grow), etch (remove), or dope (modify) the base material of the substrate These steps are repeated throughout the manufacture of a modern integrated circuit (IC) and account for over a third of the hundreds of fabrication steps involved in making an IC [2]

2.1 Plasma Processing

Plasma Enhanced Chemical Processing (PECP) takes advantage of the high-energy electrons present in glow discharges to dissociate and ionise the molecules of the gas to form chemically reactive radicals and ions The chemical processes occurring in plasmas are driven by the energy of the electrons and are not based on nor controlled by the temperature of the gas mixture or of the treated surface [1,8] The high-energy electrons can transform a normally inert gas into a highly reactive medium than then reacts with the surface of the substrate [1,2] Because of these conditions, thermal energy is not required to break chemical bonds and reactions can be promoted at low temperatures This non-thermal, non-equilibrium process has the unique property of efficiently generating chemically reactive species at low temperatures It is, therefore, possible to process substrates that do not have the thermal stability to withstand processing at higher temperatures [1]

All plasma enhanced chemical processes are the result of chemical reactions, the main difference between the various processes being the state of the final product The main steps and the plasma processes used in the manufacture of semiconductors can be summarised as

1 **Cleaning** - used to remove photoresist, residual organics, residual metallic contaminants, and native oxides or other oxides from the surface of the silicon surface The cleaning plasma produces volatile products that convert the contaminants on the surface into gaseous oxides of carbon and other gaseous products *Ashing* is a specific wafer cleaning process used for the removal of organic materials from inorganic materials

2 **Oxidation** - used to grow oxide films on metal or semiconductor surfaces An oxygen plasma is normally used and the substrate may or may not be biased Non-biased oxidation is referred to as *Plasma Oxidation* whereas biased oxidation is referred to as *Plasma Anodisation*

3 **Etching** - used for transferring a pattern to the silicon substrate The pattern to be transferred is defined by mask prepared by lithographic techniques on layers of photoresist Plasma etching is performed using reactive atoms and radical species that react with the surface to form volatile compounds that evaporate from the surface leaving an etched substrate Plasma etching has developed into several different processes such as *Plasma Etching*, *Reactive Ion Etching*, and *Magnetically Enhanced Reactive Ion Etching*

4 **Deposition** – used to create or grow many different types of films on the wafer surface including insulators, semi-conductors and metals The range of plasma-deposition processes is broadly divided into two areas Plasma-Enhanced Chemical Vapour Deposition (PECVD) and Sputter Deposition

Figure 2 1 shows a typical set of steps to create, for example, a metal film etched with submicron features on a silicon wafer substrate In (a), the metal film is deposited, in (b), a photoresist layer is deposited over the film and in (c), the photoresist is selectively exposed using the desired pattern After this, in step (d), the resist is developed, removing the exposed photoresist regions and leaving behind a patterned photoresist mask During step (e), the pattern is transferrred into the film by an etch process while the remaining photoresist protects the underlying film from being etched Finally, in (f), the remaining photoresist is removed Of these six steps, plasma processing is generally used for steps (a) and (e), and may be used for steps (d) and (f) [2]

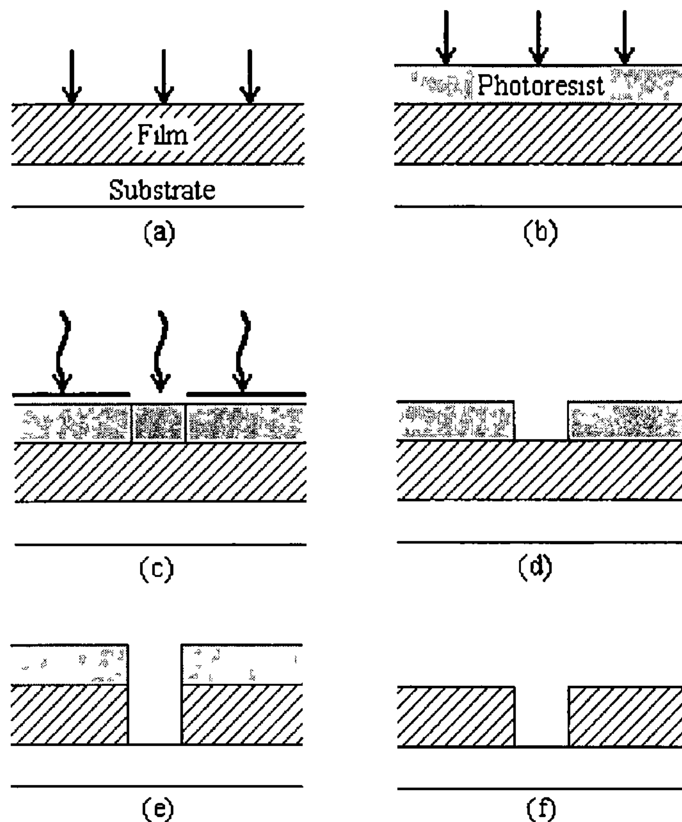

Fig 2 1 – Deposition and pattern transfer in manufacturing an integrated circuit

2.2 Plasma Process Reactors

The most common types of low-pressure plasma discharges for materials processing are those sustained by radio-frequency (RF) currents and voltages Two classes of RF plasma discharges are presently used, the capacitively coupled and inductively coupled RF plasmas RF generators are used to drive the discharges, the most widespread frequency being 13 56MHz In the manufacture of semiconductors, the wafer or substrate is placed on one electrode (which can be either grounded or biased by a second RF source), precursor gases flow through the discharge, and depleted gases are removed by a vacuum pump Figure 2 2 shows a block diagram of a plasma system used for material processing

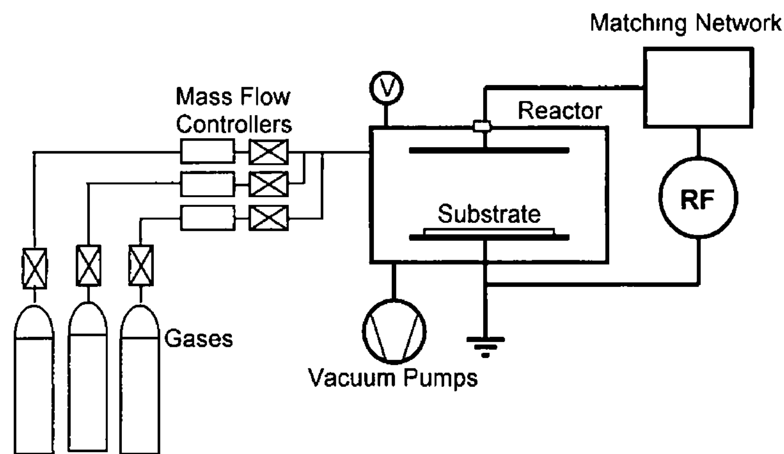

Fig 2 2 – Outline of Plasma System for Material Processing

2.2 1 Capacitive RF Process Reactors

The basic capacitive reactor, or so-called RF Diode, consists of a voltage source that drives RF current through a low-pressure gas between two parallel plates or electrodes Figure 2 3 shows a capacitive plasma chamber, called a Remberg reactor, which is used for materials processing The radial flow of the gas assists in uniform processing of the wafers

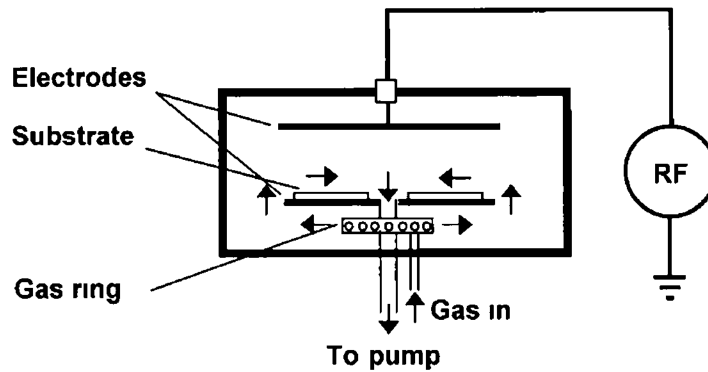

Fig 2 3 - Capacitive RF process reactor

The RF driving voltage, V_{rf}, is typically in the range 100V to 1000V, with an electrode spacing of 2cm to 10cm Typical pressures are in the range 10mTorr to 100mTorr giving plasma densities of 10^9 - 10^{11} cm^{-3} The electron temperature is of order 1eV to 20eV and ion acceleration energies (sheath voltages) are high, usually greater than 200V [2,3,7] When operated at low pressure, with the wafer mounted on the powered electrode and the plasma used to remove substrate material, such reactors are commonly called Reactive Ion Etchers (RIE's)

Increasing the RF driving voltage will increase the flux or density of ions but such a procedure is inevitably accompanied by an unwelcome increase in the energy of the bombarding ions, which can result in substrate damage Herein lies the intrinsic disadvantage of the capacitively coupled RF plasma as a source of processing plasma - the flux and energy of the bombarding ions cannot be varied independently [2,13,14]

Various methods exist which improve the performance of the common RF diode system by serving to increase or control the ion bombarding energy independently of the ion and neutral fluxes Some control over the ion-bombarding energy can be achieved by placing the wafer on the undriven electrode and independently biasing this electrode with a second RF source [2,8] Normally, this second RF source is at a different frequency than the RF source used to generate the plasma, and serves to control the sheath potential Although RF triode systems are in use, processing rates are still low at low pressures and sputter contamination is an issue

Magnetically enhanced RF diodes and triodes have also been developed These include, for example, Magnetically Enhanced Reactive Ion Etchers (MERIEs) or RF Magnetrons [7,9,14], in which a dc magnetic field is applied parallel to the powered electrode on which the wafer sits The magnetic field increases the efficiency of power transfer from the source to the plasma and also enhances plasma confinement This results in a reduced sheath voltage and an increased plasma density

2 2 2 Inductive RF Reactors

The limitations of RF diodes and their magnetically enhanced variants have led to the development of a new generation of low pressure, high-density RF plasma sources for improved process rates [1,2,8,20,23] A common feature of these sources is that the power (RF or microwave) is coupled to the plasma across a dielectric window [9,10,15], rather than by direct connection to an electrode in the plasma This non-capacitive power transfer is the key to achieving low sheath voltages and hence, low ion acceleration energies, at all surfaces [2,4,9] To control the ion energy, the electrode on which the wafer is placed can be independently driven by a capacitively coupled RF source Hence, independent control of the ion flux (through the source power) and energy (through the wafer electrode power) is possible [8,10,18]

In an RF inductive discharge the plasma acts as a single-turn, lossy conductor that is coupled to a multi-turn non-resonant RF coil RF power is inductively coupled to the plasma by transformer action RF current passing through the coil produces an oscillating induced electric field that is capable of generating and maintaining a plasma [9,10,16,21,22,30]

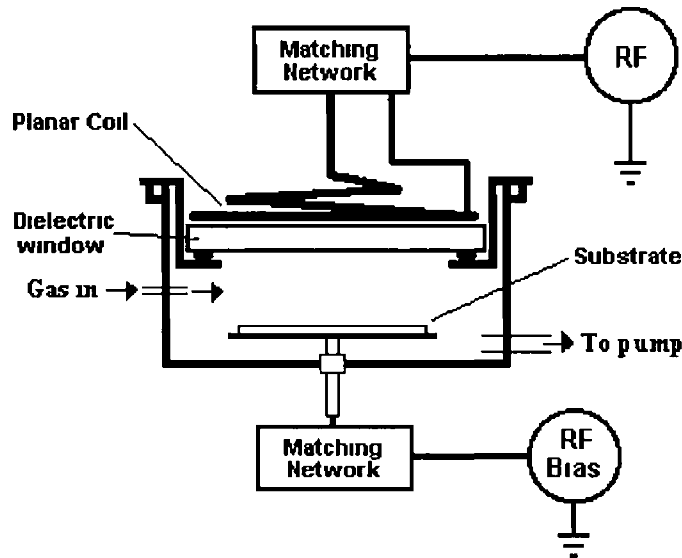

Fig. 2 4 – Planar Inductive RF process reactor

Two coil configurations, cylindrical and planar, are possible The planar coil [11,12] is a flat helix wound from near the axis to near the outer radius of the discharge chamber, as shown in Figure 2 4 Multipole permanent magnets can be used around the process chamber to increase the radial uniformity of the plasma [10,14] The planar coil can also be moved closer to the wafer surface, resulting in a close-coupled or near-planar source geometry having good uniformity properties even in the absence of multipole confinement The planar coil configuration is the most common type of inductively coupled plasma source used in materials processing It is capable of high density (10^{10} - 10^{12} cm^{-3}), low pressure (<50mTorr) discharges [10,13,14,20,22]

Although the RF driving voltage (at the high voltage end of the coil) is comparable to that of capacitive discharges, only a small fraction of the voltage appears across the sheath, such that the ion energy loss is considerably lower Hence, the inductive discharge is significantly more efficient than the capacitive discharge [9,14,16] In high-density inductive discharges, the sheath thickness, and hence, sheath capacitance, is much smaller than that in capacitive discharges due to the higher electron density [1,2] Therefore, the sheath voltage is much smaller in an inductive discharge as a result of the capacitive voltage divider effect of the plasma and sheath capacitance's [2]

Chapter 3

PLASMA IMPEDANCE MONITOR

The *Plasma Impedance Monitor* (PIM) is an RF impedance probe that measures the amplitude and phase of the first five Fourier components (harmonics) of the plasma voltage and current The PIM consists of a novel Current/Voltage Sensor (IV Sensor) and state-of-the-art data acquisition electronics (RF Vector Integrator) The RF Vector Integrator is contained within a 19" rack case that also includes an IBM compatible embedded PC This assembly is referred to as the embedded system A standard PC (Host PC) is connected to the embedded system using an RS232 link Software executed on the embedded PC controls the RF Vector Integrator and communicates with the host PC The host PC is used mainly to display the plasma parameters calculated by the software analysis routines of the embedded system A typical process chamber set-up using the PIM is shown in Figure 3 1

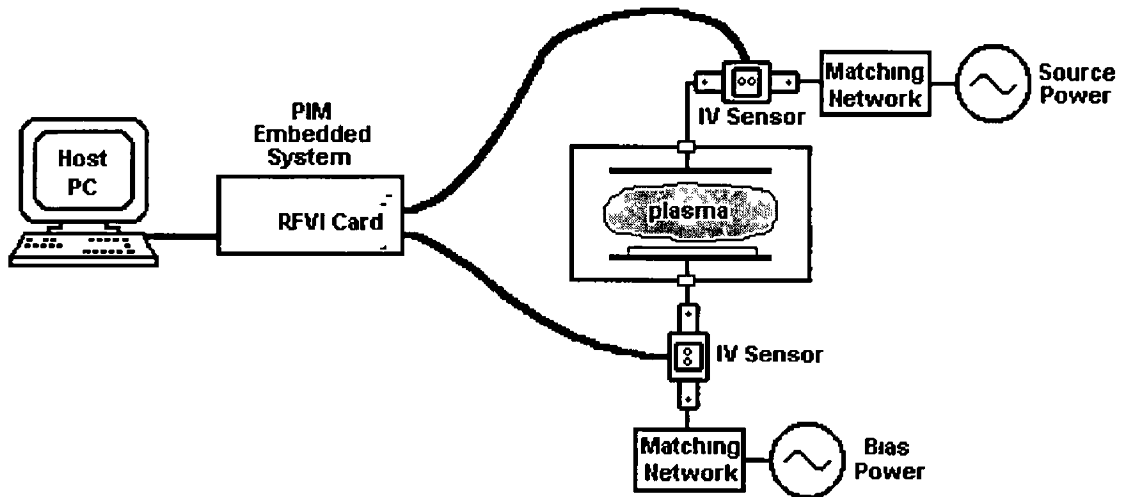

Fig 3 1 – Typical Installation of the PIM System

3.1 Present Measurement Techniques

In principle, voltage and current measurements are straightforward Some techniques involve either commercial or custom built probes using expensive measuring equipment [19,28,35,42,43] The most successful methods digitise the sampled RF current and voltage waveforms and analyse the digitised waveforms using digital signal processing techniques to extract the required parameters However, the low-bit resolution of present time high-speed analogue-to-digital converters results in inadequate accuracy and precision required for plasma diagnostics In addition, the requirement for extremely fast RAM to store the digitised waveforms makes such a system expensive

In practice, the main technical difficulties with RF current and voltage sensors are due to inadequate shielding of the current and voltage sensors from stray magnetic and electric fields The most critical of these effects is that on the calculation of power due to phase measurement errors [18, 19] For example, an error of 0 5° at a phase angle of 88° results in a 20% to 25% error in the calculated power [18]

3 1 1 Conventional IV Sensor

The standard approach to sensing the current and voltage delivered to the process chamber is shown schematically in Figure 3 2 The RF Current is measured by a single loop current sensor and the RF Voltage by a capacitive pickup placed near the RF power conductor [19]

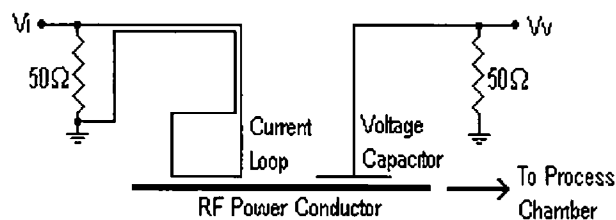

Fig 3 2 - Conventional RF Current/Voltage Sensor

The voltage sensor is capacitively coupled to the RF power conductor and is terminated by a 50Ω resistance The electric field generated by the RF voltage on the power conductor between the sensor and the power conductor results in a charge being developed on the voltage sensor The charge is related to the capacitance between the sensor and the power conductor, and to the RF voltage This charge results in a voltage being developed across the terminating resistance that is given by the equation [19,33,34]

$$V_v = RC\frac{dV_{rf}}{dt} \tag{3 1}$$

where V_v is the voltage produced by the voltage sensor,
V_{rf} if the RF voltage on the RF conductor,
C is the capacitance between the sensor and the RF conductor,
R is the value of the terminating resistance

The current sensor is inductively coupled to the RF power conductor and is also terminated by a 50Ω resistance The magnetic flux created by the RF current flowing in the power conductor induces a current in the sensor The induced current is related to the mutual inductance between the loop and the power conductor, and to the RF current This current then develops a voltage across the terminating resistance that can be represented by the equation [19,33,34]

$$V_i = M\frac{dI_{rf}}{dt} \tag{3 2}$$

where V_i is the voltage produced by the current sensor,
I_{rf} if the RF current flowing in the RF conductor,
M is the mutual inductance between the loop and RF conductor,
R is the value of the terminating resistance

The main problems with this standard type of sensor are:

- electric fields generated by unrelated sources can cause stray voltages to be added to the signals measured by the sensing elements (stray voltage pickup or cross-talk)
- spurious magnetic fields can cause a stray current to be induced in the current sensing loop (stray field pickup)
- physical separation between the current and voltage sensor locations result in a phase error

3.1.2 PIM IV Sensor

The IV sensor used with the PIM was designed to overcome some of the problems associated with conventional methods of sensing the RF current and voltage, and has been granted a US patent [39]. The design is shown schematically in Figure 3.3. The IV sensor contains a unique current sensing loop and a conventional voltage pickup sensor fabricated on a PCB that is contained with a PTFE block, as shown in Figure 3.4.

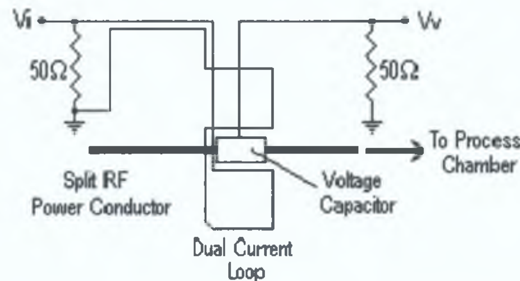

Fig. 3.3 – Schematic of PIM IV Sensor

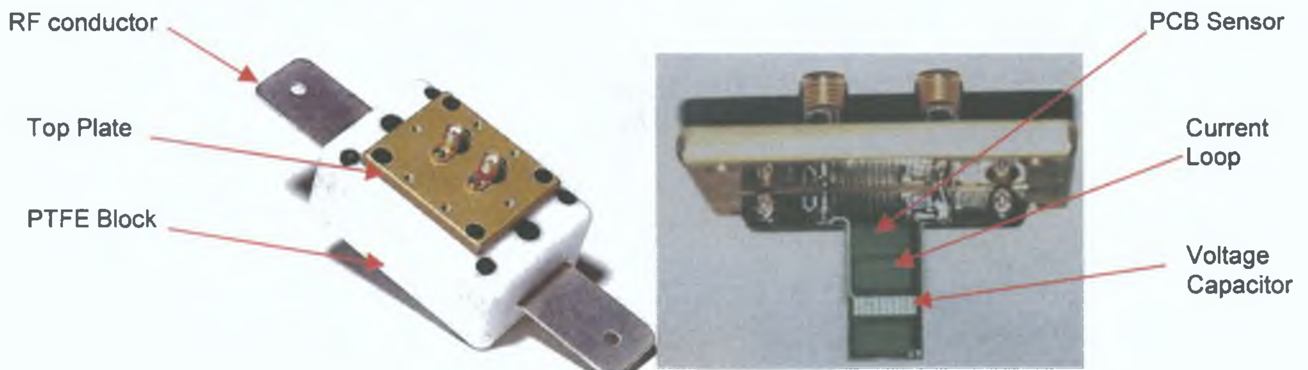

Fig. 3.4 – PIM IV Sensor and Sensor PCB

The RF power conductor is divided into two equal parts along its length so that the same quantity of the RF current flows in each part. The current sensor consists of two loops of equal area that are connected in a figure-of-eight configuration. This sensor is located in the gap between the two divided parts of the RF conductor, as shown in Figure 3.5. The sensor is positioned so that the loops are symmetrically located on each side, top and bottom, of the RF conductor. The voltage sensor is a small capacitor positioned between the loops of the current sensor, and is also located symmetrically about the centre line of the RF power conductor.

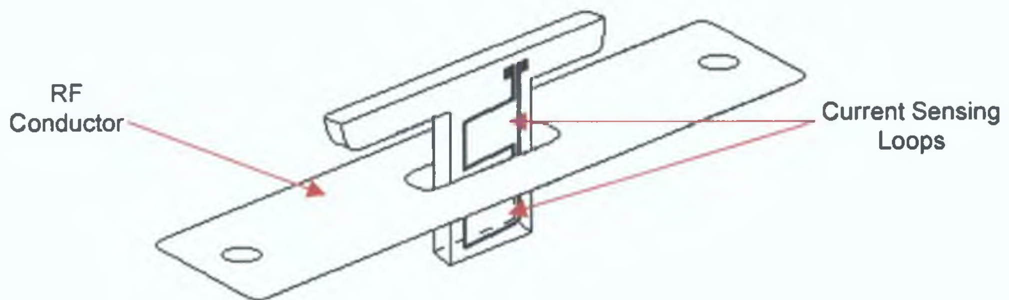

Fig. 3.5 –RF Power Conductor and Sensor PCB Location

The magnetic field created by the RF current flowing in the power conductor induces an equal current in each loop of the current sensor. The induced currents are of opposite direction but the figure of eight configuration results in the induced currents being added together. However, any induced currents due to stray magnetic fields normal to the direction of RF current flow will be induced in each loop equally and in the same direction, and so, will cancel each other out. A third current sensing loop (not shown in Figure 3.3) is also connected to the figure-of-eight loops so that any current induced by stray magnetic fields parallel to the direction of RF current is also eliminated.

To reduce the effects of stray voltage pickup or cross talk, a grounded shield protects the loops of the current sensor. This shield acts as a Faraday shield and reduces the amount of voltage pickup that the loops detect. Finally, there is minimum phase error between the current and voltage sensors since both sensors are located at the same position in the centre of the RF conductor.

3.2 Waveform Sampling

The most common frequency used to drive semiconductor process plasmas is 13 56MHz To sample the signals produced by an IV sensor in such an environment, a data acquisition system with a sampling frequency of approx 135 6MHz would be required if measuring up to the fifth harmonic This is based on the Nyquist sampling theorem Aliasing has been used as a sampling technique to reduce the sample rate to sub-Nyquist frequencies This technique allows high bit ADCs and low cost RAM to be used to improve the accuracy and precision of the measurements The technique produces a replica of the RF current and voltage waveforms at much lower frequencies than that of the actual waveforms [35]

The PIM RF Vector Integrator uses a novel sampling technique called *Coherent* sampling to achieve the same results The sampling technique developed is immune to changes in the frequency of the sampled RF current and voltage waveforms and requires very little RAM to store the digitised waveforms In addition, the amplitude and phase resolution are significantly improved This design has been granted a US patent [53]

3 2 1 Coherent Sampling

The Nyquist theorem states that a waveform must be sampled at least twice as fast as the highest frequency component of the waveform Or, in other words, the highest frequency component cannot exceed one half of the sample rate [36,37] Coherent sampling is a novel technique that allows sampling of a waveform with a sampling frequency below the Nyquist frequency of the waveform

During coherent sampling, a set of sample points is recorded at specific time intervals, and over a number of cycles, of the repetitive signals as generated by the IV sensor The sampling frequency is chosen so that the time interval between sample points results in one cycle of the waveform being fully sampled after an integer, N, number of cycles has elapsed When the sampling process is complete, it is necessary to organise the sample points into their corresponding phase locations to correctly reconstruct the sampled waveform The phase locations of successive sample points

reconstruct the sampled waveform The phase locations of successive sample points will exactly match the phase locations of previous sample points after N cycles of the waveform has elapsed

With coherent sampling, the sample frequency can be arbitrarily chosen and does not have to meet the Nyquist criteria There is no loss of information of the signal being sampled as long as the bandwidth of analogue circuitry of the sampling system exceeds that of the signal being sampled The sampling frequency, Fs, is given by

$$Fs = F(M/N) \tag{3 4}$$

where F is the fundamental frequency of the waveform being sampled, M and N are integers

This means that the waveform will be sampled M times over N consecutive cycles of the waveform If M and N have no common factor, all the samples measured during the N consecutive cycles will be at unique positions on the waveform That is, the sample points all have a unique phase relationship relative to the waveform

Figure 3 7 shows a repetitive waveform being sampled using coherent sampling If, for example, the fundamental frequency of the waveform is 2MHz, and the values of M and N are 10 and 3 respectively, the sampling frequency is approx 6 67MHz Figure 3 8 shows one cycle of the signal after the sample points have being re-organised into their respective phase locations

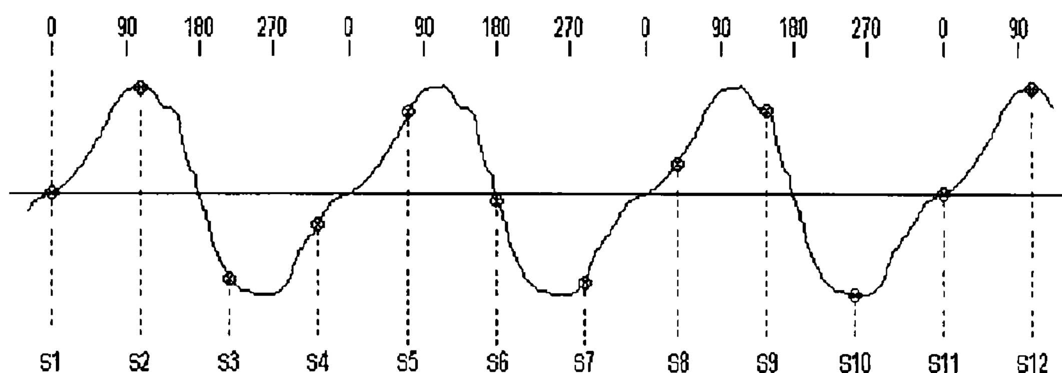

Fig 3 7 – Sample Points of a Repetitive Waveform generated by Coherent Sampling

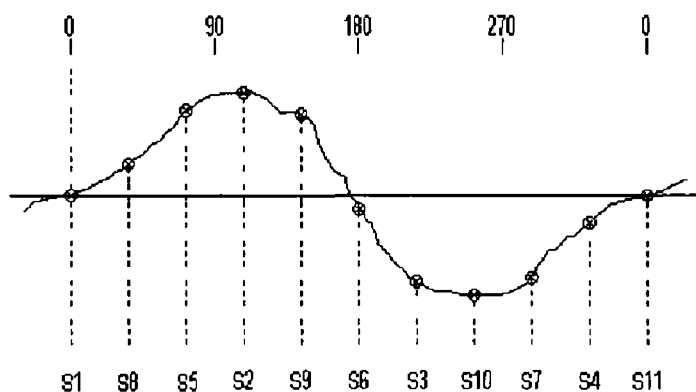

Fig 3 8 – Reconstruction of one cycle of the Repetitive Waveform

In this example, the sample points and their phase locations are as follows

Sample Point	Phase Location
S1	0°
S2	108°
S3	216°
S4	324°
S5	72°
S6	180°
S7	288°
S8	36°
S9	144°
S10	252°
S11	0°

For this example, the highest frequency component of the waveform that can be distinguished (using the Nyquist criteria) is calculated as follows

Fundamental Frequency = 2MHz
Sampling Frequency Multiplier, M = 10
Effective Nyquist Sampling Frequency = 2MHz X 10 = 20MHz
Highest Frequency Component = 10MHz

Therefore, although the waveform is sampled with a frequency below the Nyquist frequency, coherent sampling effectively and efficiently implements Nyquist sampling With coherent sampling it is possible to use high bit digitisers to increase the SNR since sub-Nyquist sampling frequencies can be used In addition, a relatively low

quantity of RAM is required to store the sample points since the number of sample points required is simply the sampling frequency multiplier, M

For a plasma discharge driven by a frequency of 13 56MHz, coherent sampling can be implemented with the following characteristics to record up to the fifth harmonic

Fundamental Freq	= 13 56MHz
M/N	= 10/23
Sampling Freq	= 5 89MHz
Effective Nyquist Freq	= 135 6MHz
Highest Freq Component	= 67 8MHz
SNR	= 62dB (10-bit ADC)
SNR	= 74dB (12-bit ADC)

3 2 2 Signal Averaging

To improve the accuracy of the sampled points, signal averaging can be used Signal averaging allows a signal that is composed of a periodic or repetitive waveform and non-coherent noise to be recorded more accurately Averaging improves the signal-to-noise ratio (SNR) of the sampled signal by the square root of the number of averages performed [36] The theoretical SNR of a signal sampled using Nyquist sampling can be calculated from [38,44]

$$SNR = (6\ 02N + 1\ 76)\ dB \qquad (3\ 3)$$

where N is the number of ADC bits

For example, a signal with a fundamental frequency of 13 56MHz sampled using an 8-bit ADC would give a SNR of 50dB, if recording the fifth harmonic By using coherent sampling, a 10-bit or 12-bit converter can be used because the actual sampling frequency is sub-Nyquist An improvement of 12dB or 24dB in the theoretical SNR as compared to an 8-bit converter can then be achieved That is, there is an improvement factor of between 4 and 16 in the SNR if using 10- or 12-bit converters rather than an 8-bit converter However, with coherent sampling, the phase locations of successive sample points will exactly match the phase locations of previous sample points after N cycles of the waveform have elapsed Therefore, signal averaging can be used to increase the SNR even further

3.3 RF Vector Integrator Card

The PIM RF Vector Integrator (RFVI) is shown in the block diagram of Figure 3 9 It consists of two identical waveform sampling channels, one each for the current and voltage signals, and is a high frequency, high-resolution system that uses coherent sampling The circuit was fabricated on a full-size PC ISA printed circuit board, as shown in Figure 3 10

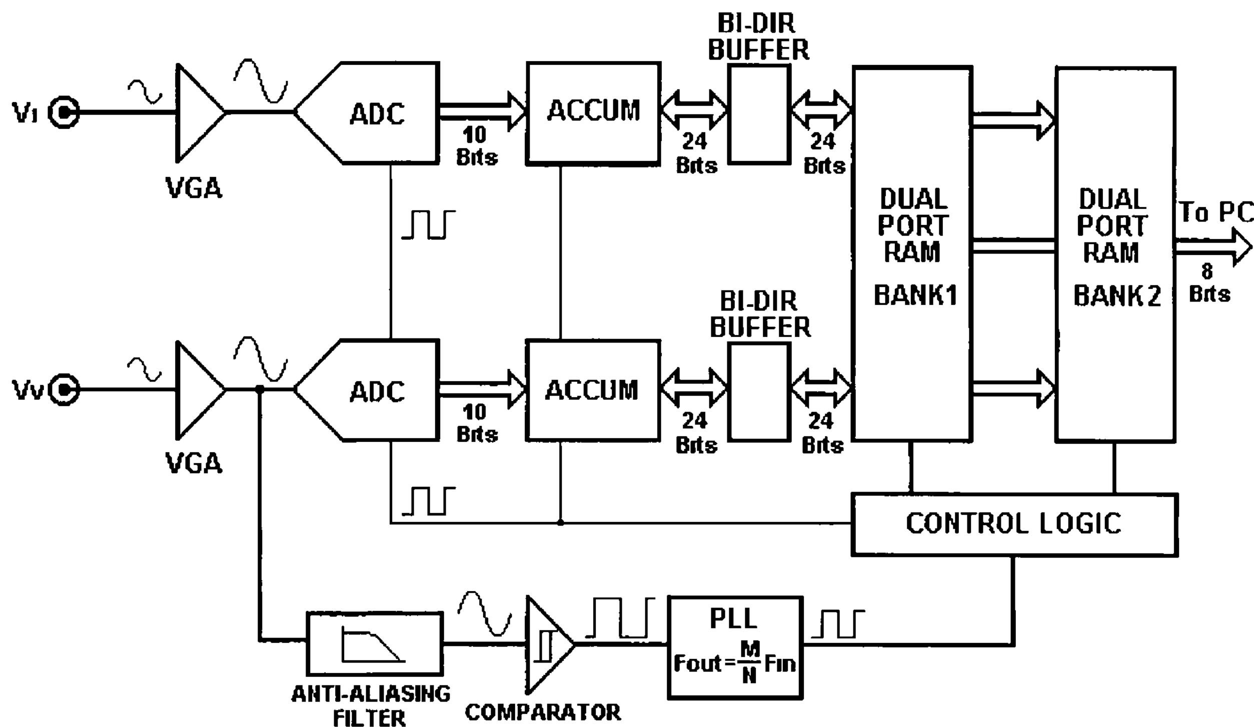

Fig 3 9 – PIM Waveform Sampling Circuit

The RFVI card contains a front-end analogue circuit that consists of two variable gain amplifiers, or VGA's, and two 10-bit sample-and-hold type analogue-to-digital converters, or ADC's The digitised data from the ADC's is passed to a digital circuit that consists of two 24-bit accumulators and two banks of 24-bit wide dual port RAM In addition, the signal in the Voltage channel is used with a clock generation circuit to produce the sampling clock and other higher frequency clocks required by the digital circuit The 24-bit accumulators and RAM allow up to 2^{14}, or 16384, averages of the 10-bit words to be performed This can, theoretically, give an improvement in the SNR of up to 42dB, yielding an overall SNR of up to 104dB or an equivalent resolution of 17-bits

Fig. 3.10 – PIM RF Vector Integrator Card

3.3.1 Principle of Operation

The VGA's either amplify or attenuate the signals produced by the IV Sensor, which are then passed to the ADC's where they are converted to 10-bit words. The 10-bit digitised sample points are passed to the 24-bit accumulators where they are added to previous sample points with identical phase relationships that are stored in the dual-port RAM. The sample points are stored in the order in which they are processed in the RAM. The digital logic that controls the dual-port RAM also incorporates a Look-Up-Table, or LUT, to control the addressing of the RAM so that the sample points are stored in their correct phase order.

To generate the required coherent sampling clock signal, the Voltage signal is also passed to the clock generation circuit. The first stage of this circuit consists of a low-pass or anti-aliasing filter that eliminates any frequency components in the signal above the fundamental frequency. This is required to prevent higher frequency components in the signal generating a sample clock higher in frequency than that required. The sinusoidal Voltage signal is converted to square wave, or clock, signal that is then input to a Frequency Generator Phase Locked Loop (PLL). The PLL generates an output clock signal that has a fixed phase relationship to the input clock signal. In addition, the output clock frequency is determined by programming the PLL with a multiply, M, and divide, N, value. This provides an output clock at a frequency that is phase locked to the input clock and is proportional to the frequency of the input clock. Therefore, the sampling clock, which is the output clock of the PLL, can sample

the IV Sensor signals coherently, regardless of variations in the fundamental frequency of the signals

To utilise the full potential of the RFVI card, the gains of the VGA's are adjusted to keep the signal level at the inputs of the ADC's within specific levels The VGA's used have a gain range of between –11dB to +30 dB with a bandwidth of 90MHz The gain accuracy of the VGA is ±0 5dB Applying a differential DC voltage to the Gain Control inputs of the VGA sets the gain The control voltage variation is ±500mV and is generated by an 8-bit digital-to-analogue converter, or DAC, with a full-scale output of 2 55V (10mV/bit) This results in a gain-setting resolution of 0 2dB/bit when using a divider ratio of 2 with the DAC

Two main problems exist with the VGA's The first problem is that the gain error is periodic with the gain control voltage to approximately ±0 5dB This can result in variations in the output signal level of the VGA The second problem is that the group delay of the amplifier varies with the control voltage If the two VGA's have different gains, one signal will be delayed more than the other and this would result in a phase error To overcome these problems, the VGA's are operated with four gain settings The actual gains used were calculated to obtain sufficient resolution with the ADC's, with the VGA's being calibrated for both gain and group delay

The process of Coherent Sampling and accumulation can continue indefinitely The RFVI card contains two banks of dual-port RAM Only one bank at a time is used during the sampling and accumulation process, while the other bank is free to be read and analysed by the control software When one bank has filled its memory locations, the control logic seamlessly switches the banks so that the cleared bank is now used for the sampling and accumulation process leaving the other bank free The ability to switch banks without stopping and restarting the sampling and accumulation process means that the circuit can continuously collect data, maximising the SNR and eliminating dead-time For a complete circuit diagram of the PIM RFVI card, refer to the circuit schematic diagrams in Appendix A

3 3 2 System Software

Two specific software applications were developed for the PIM system The first software developed is used to set-up and control the RF Vector Integrator card installed in the embedded system It also calculates the phase and amplitude of the Voltage and Current signals acquired by the card for all harmonics This software is referred to as the embedded software, or *PIMCode* The second software developed is a Windows 95™ based application that is a user-friendly environment for displaying, recording, or further processing the signal values calculated by the embedded system This software is referred to as the host software, or *PIMSoft*

PIMCode is executed on the processor card of the embedded system The control routine initialises and enables the process of coherent sampling and also automatically adjusts the gains of the VGA's so that the optimum ranges of the ADC's are used The analysis routine performs a Discrete Fourier Transform, or DFT, on the digitised sample points stored in the RAM of the card The DFT provides amplitude and phase information for each harmonic of the Voltage and Current signals digitised by the RF Vector Integrator card

PIMSoft is executed on a standard PC as a Windows 95™ application It communicates with the embedded system via an RS232 serial communications link It allows the user to either graph the data generated by the embedded system or simply display the present values in a meter-type window It also allows the data to be automatically saved to the hard disk of the PC for future analysis or comparison

Chapter 4

PIM CALIBRATION

The PIM ıs a hıgh-resolutıon system that requıres careful and accurate calıbratıon There are two stages to the PIM calıbratıon procedure The first stage ıs the calıbratıon of the RFVI and the second stage beıng the calıbratıon of the IV Sensor Thıs second stage ıs accomplıshed usıng the calıbrated RFVI card

As there ıs no standard ınstrument comparable to the PIM system, ıt ıs necessary to use secondary ınstruments to calıbrate the PIM The most unıversal and acceptable method of verıfyıng the calıbratıon and accuracy of an ımpedance probe ıs that of RF power measurement ın a 50Ω envıronment If accurate power measurement can be proved, the basıc RF measurements of Voltage, Current and Phase must be correct The power ıs calculated by

$$P = VI\cos\phi \qquad (3\ 1)$$

where V = voltage
I = current
ϕ = phase between voltage and current

Thıs, however, ıs only true ıf at least two of the basıc measurements can be proven to be accurate For example, ıt ıs possıble to calculate the rıght value of power ıf, say, the voltage and current measurements are ınaccurate by 2% That ıs, ıf the voltage ıs measured at 2% below the correct value and the current as 2% above the correct value, then the calculated power wıll stıll be correct Wıth thıs ıs mınd, a NIST traceable RF power meter ıs used for power measurement and an oscılloscope ıs used for RF voltage measurement In addıtıon, a commercıal ımpedance meter ıs used to measure the ımpedance of the RF load

4.1 RF Vector Integrator Calibration

To calibrate the RFVI card a stable sinusoidal signal is injected into both the inputs of the card simultaneously The signal amplitude is set to the lower and upper limits of each gain range that the card uses and the magnitudes of the fundamental values (Voltage, Current and Phase), as measured by the PIM, are recorded The same signal amplitudes are then measured by a calibrated oscilloscope Amplitude and phase calibration figures for each gain range are then calculated Figure 4 1 shows the set-up used to calibrate both channels of the RFVI card A graph showing the relationship between the RFVI card measurements and the scope measurements after the RFVI card has been calibrated is shown in Figure 4 2

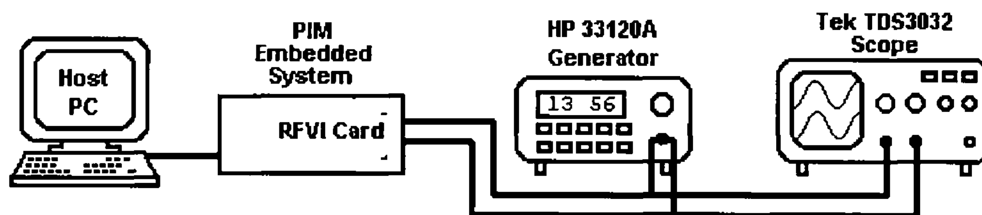

Fig 4 1 – Amplitude Calibration of RF Vector Integrator

The signal source used was a HP 33120A Waveform Generator It is capable of generating sinusoidal signals of between 18mV$_{RMS}$ and 3 5V$_{RMS}$ into a 50Ω termination This adequately covers the full range that the RFVI card was designed to measure The oscilloscope used for voltage measurement was a Tektronix TDS3032 DPO oscilloscope It is a 9-bit digital storage oscilloscope with a measurement accuracy of ±2% of its measurement

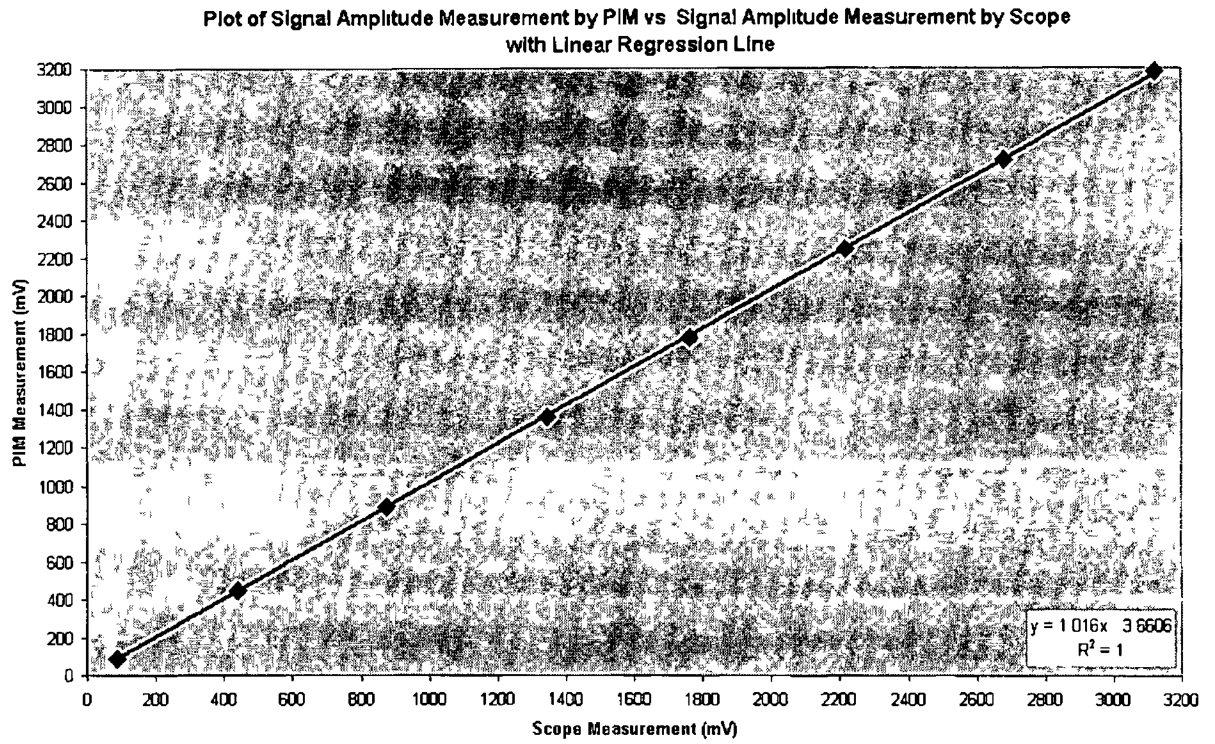

Fig 4 2 – Graph of RFVI Card Measurements vs Scope Measurements

4.2 IV Sensor Calibration

To calibrate the IV Sensor, the sensor is installed into a RF circuit and its response at various values of power and load impedance is recorded Initially, the load is set to 50Ω resistive (phase is zero) This condition is verified with a Hewlett Packard 4193A Impedance Meter RF power is passed through the circuit and the fundamental values of Voltage, Current and Phase are measured using the previously calibrated RFVI card An oscilloscope is used to measure the actual RF voltage By measuring the load and actual RF voltage, the RF current is calculated using Ohm's Law Calibration figures for the IV Sensor are then calculated

Once the initial calibration at 50Ω is complete, the load impedance is changed to a capacitive load and then to an inductive load Measurements at low power values (to prevent damage to the loads) are recorded using the PIM system and again, the scope is used to measure the RF voltage as an absolute check The reference power sensor is not used with these loads because it cannot accurately measure power with non-50Ω loads The sensor calibration set-up is shown in Figure 4 3 A graph of the PIM power measurements and the reference power measurements are shown Figure 4 4

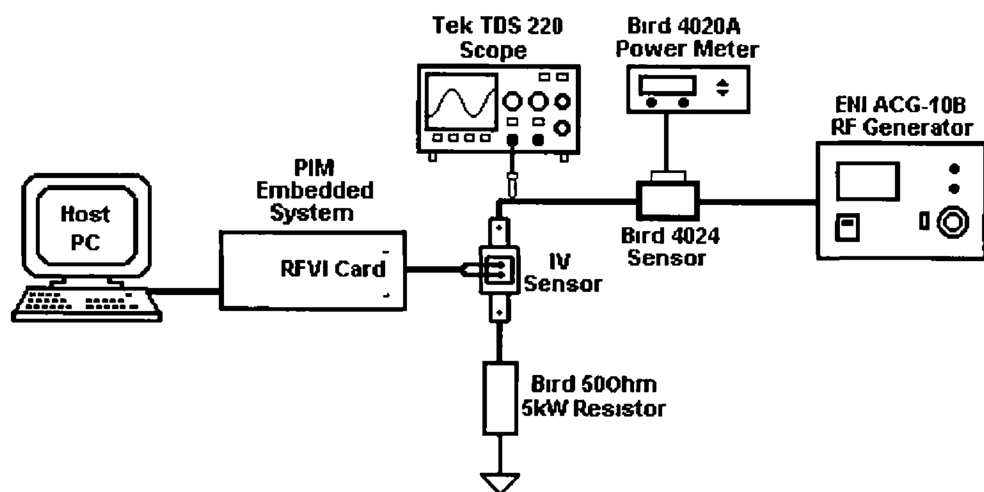

Fig 4 3 – Calibration of IV Sensor

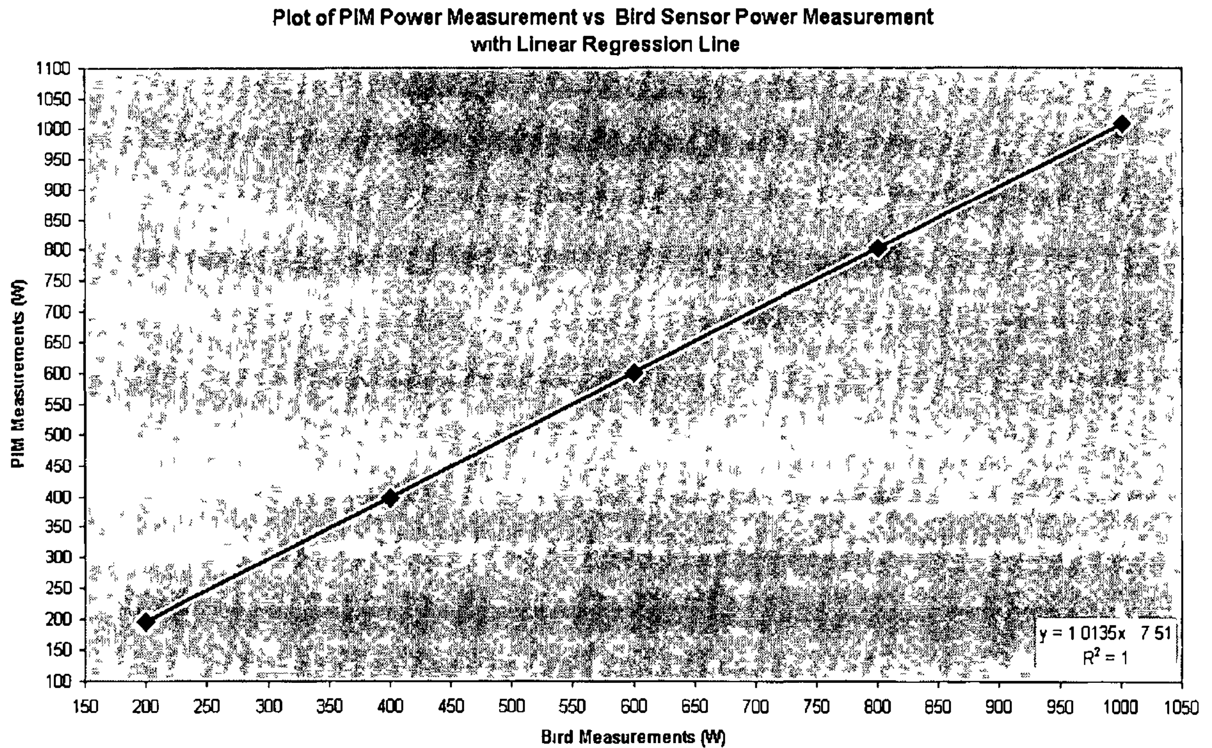

Fig 4 4 – PIM Power Measurement vs Bird Sensor Power Measurement

The reference power sensor used was a Bird 4024 RF Power Sensor and Bird 4020A Power Meter It is calibrated to NIST standards and is capable of measuring RF power between 3W and 10kW within a frequency band of 1 5MHz to 32MHz The accuracy of this instrument is ±3% of its reading (at its maximum range) The oscilloscope used for voltage measurement was a Tektronix TDS 220 oscilloscope It is an 8-bit digital storage oscilloscope with an accuracy of ±2% of its measurement, and is capable of voltage measurements up to 150V_{RMS} Finally, the RF generator used was an ENI ACG-10B 1kW 13 56MHz generator

Calibration figures relating to the RF Vector Integrator and IV Sensor are recorded in separate files on the embedded system, and are used by the analysis routines of PIMCode

4.3 Testing

Testing of the PIM involves installing the IV Sensor in a test rig that can simulate, to a certain extent, the RF electrical properties of a plasma To this end, a test rig called a Dynamic Dummy Load, or DDL, is used The DDL consists of two identical Capacitor-Inductor networks that are connected to a RF power source and a 50Ω power resistor A schematic diagram of the DDL is shown in Figure 4 5

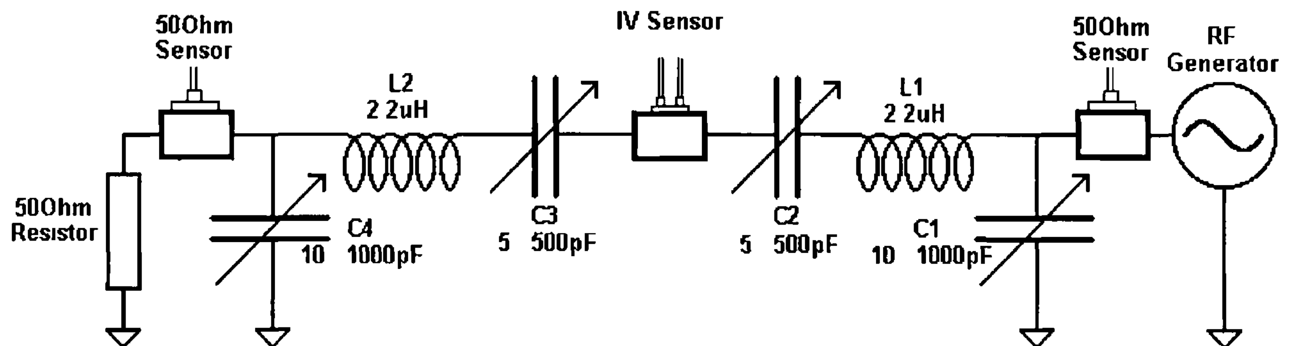

Fig 4 5 – Plasma Simulation Rig, or DDL

The IV Sensor is installed between the Capacitor-Inductor networks of the DDL The Capacitor-Inductor network that is connected to the RF generator is referred to as the Match and the second network as the Load This circuit is electrically similar (in terms of fundamental parameters) to a plasma processing system with the Load network acting as the plasma By varying the settings of the Load capacitors, it is possible to simulate a wide range of plasma RF conditions, in terms of the fundamental RF Voltage, Current and Phase The Match is adjusted to minimise the amount of reflected power at the RF generator 50Ω power sensors are located at the input and output of the Match and Load networks respectively It is assumed that the power loss in the networks is negligible, as their construction is identical, but it is conceivable that non-equal power loss will occur Unfortunately, it was not possible to measure or determine the actual power loss Therefore, the power that passed through the IV Sensor is assumed to be the average of the input and output powers as measured by the 50Ω sensors, with any reflected power taken into account

The capacitors and inductors of the Match and Load networks are contained within aluminium boxes and are fitted with dials that are used to set and record their positions. The power sensor input and output connectors of the Match and Load networks use N-type bulkhead connectors with N-type cable being used with the RF generator and load resistor. The IV Sensor is fixed to rectangular metal straps that connect to the series capacitors of both networks. The top plate of the IV Sensor is secured to an aluminium plate that is connected between both networks. A photograph of the DDL test rig is shown in Figure 4.6.

Figure 4.6 – DDL Test Rig

A set of measurements taken with a PIM system using the DDL is given in Table 4.1. The generator used with the DDL was an ENI ACG-10B 1kW 13.56MHz RF generator. The reference powers were measured using Adtec 50Ω power meters. The Adtec system allows the measurement and display of the forward and reflected powers of both sensors simultaneously. It was assumed that the power that passes through the PIM IV sensor is the average of the input and output powers of the DDL as measured by the Adtec sensors. It should be noted that the Adtec sensors were calibrated against a Bird 50Ω digital power sensor (model no.: 4024) using the 50Ω power resistor as a load.

The results in Table 4 1 demonstrate the range of electrical parameters possible with the DDL system It also highlights the performance of the PIM system

PIM VALUES (Fundamentals only)				ADTEC VALUES				
RF V (Vrms)	**RF I (Arms)**	**Phase (Deg)**	**Power (Watts)**	**Input Power (Watts)**	**Output Power (Watts)**	**Avg Power (Watts)**	**Power Error (Watts)**	**Power Error (%)**
207 85	5 47	-74 61	301 73	300 00	285 00	292 50	9 21	3 16
379 80	9 77	-74 70	979 14	1000 00	950 00	975 00	4 14	0 42
89 65	3 83	-31 77	291 91	300 00	292 00	296 00	4 09	-1 38
167 30	6 95	-31 64	989 91	1000 00	980 00	990 00	0 09	-0 01
125 20	2 36	0 93	295 43	300 00	295 00	297 50	2 07	-0 69
232 50	4 29	1 08	997 25	1000 00	985 00	992 50	4 75	0 48
102 90	3 82	42 40	290 27	300 00	291 00	295 50	5 23	-1 77
190 00	6 94	41 60	986 05	1000 00	974 00	987 00	0 95	-0 10
135 15	6 28	70 62	281 64	300 00	279 00	289 50	7 86	-2 72
246 80	11 15	70 29	928 08	1000 00	932 00	966 00	37 92	-3 93
							MAX	**3 16**
							MIN	**-3 93**
							MEAN	**-0 65**
							STD DEV	**1 96**

Table 4 1 – DDL Results

The powers at the high phases show higher errors than those at the lower phases It must be remembered that the PIM calculates the power using the Voltage, Current and cosine of the Phase measurements Therefore, small errors in the measurement of phase will lead to large errors in the cosine of the phase and the calculated power For example, an error of 0 5° at a phase angle of 88° results in a 20% to 25% error in the calculated power [18]

Chapter 5

PIM MEASUREMENT PERFORMANCE

To demonstrate the measurement resolution and repeatability of the PIM system, three identical sensors were installed on a plasma tool and the RF Voltage, Current and Phase at three different power levels was recorded The plasma tool was an Applied Materials DPS Centura tool which uses a 2MHz non-resonant coil to generate the plasma and has a wafer bias of 13 56MHz The sensors were used to measure the wafer bias when the power was increased from 75W to 150W and then to 225W

Calculations on the measurements, which are summarised on the following pages, were performed on the portions of the data where the measurements had stabilised (refer to Figures 5 7 to 5 9) That is, the measurements where the power was changing have been omitted in order to present a true indication of the system performance The portion of the measurements used and their corresponding power levels were

Points	**Power Step**
5 to 35	75W
60 to 75	150W
85 to 100	225W

For each RF parameter recorded, the average value for the 3 sensors was calculated The difference between the maximum and minimum of the individual sensor measurements and the average value for the 3 sensors was then calculated as a percentage of the average value In addition, the difference between the individual sensor measurements and the average value was calculated (and is shown as an absolute value) The difference in the Phase measurements is not shown as a percentage value as the real difference is a more useful parameter for representing Phase repeatability

It must be remembered when considering the following results that the measurements taken with each sensor would be prone to slight differences as it would impossible to maintain the exact same experimental conditions for each sensor Two types of error would be present It is conceivable that there would exist a "plasma repeatability error" which is due to the difference between the plasmas generated after each individual sensor has been installed on the tool In addition, there would be a "sensor repeatability error" which is the measurement error that each sensor would have due to slight calibration or installation differences between each sensor

Both these errors would result in an uncertainty as to the true value of the RF measurements made by each sensor Therefore, the measurement error is a combination of the repeatability of the sensors and the repeatability of the plasmas

Finally, the measurements shown were made possible due to the kind permission of a commercial corporation to allow this experiment to be performed Unfortunately, due to the tight constraints of access to commercial plasma process reactors, it was not possible to repeat the experiment or to perform any on-site analysis of the data captured As a result, some doubt remains regarding the sources of errors of some of the measurements and to the reproducibility of the measurements or plasma conditions

5.1 Voltage Measurement Repeatabılıty

Although the Voltage Fundamental measurements are relatıvely low (the PIM used could measure up to 2kV), good repeatabılıty can be seen The largest error ıs observed wıth the measurements of *Sensor 2*, and ıs approx 5 9% Thıs corresponds to a real voltage dıfference of 1 4V when the nomınal voltage was 23 7V The smallest error ıs also seen wıth *Sensor 2*, and ıs approx 0 13% or 51mV on a nomınal voltage of 40 5V

I cannot explaın, wıthout doubt, why the measurements at a power of 150W (especıally for *Sensor 2*) are not as repeatable as those taken durıng the 75W and 225W power steps It may be that the plasma state was not the same durıng the 150W step as at the other power steps, or that the power was not set exactly the same when the measurements wıth *Sensor 2* were performed at thıs power step From the graph shown ın Fıgure 5 7, ıt can be seen that the measurements taken wıth *Sensor 2* durıng the 150W power step devıate from those taken wıth *Sensor 1* and *Sensor 3*

Also, ıt ıs ınterestıng to note that the measurements of the Voltage 3rd Harmonıc at the 150W power step dısplay a dıfferent trend than those of the correspondıng Current measurements However, ıt should also be noted that the three sensors record sımılar trends so ıt would seem that thıs effect ıs not a sensor effect but ıs eıther due to the plasma condıtıon or due to the external RF hardware

Values for Voltage Fundamental

Power		Avg (V)	Sensor 1 % Error	Sensor 1 Abs Dıff (mV)	Sensor 2 % Error	Sensor 2 Abs Dıff (mV)	Sensor 3 % Error	Sensor 3 Abs Dıff (mV)
75W	Mın	10 78	-1 29	139 05	-1 30	139 82	-0 62	66 39
	Max	10 96	-0 26	28 53	1 59	173 86	1 60	175 74
150W	Mın	23 69	1 09	258 67	-5 89	1396 38	3 45	818 34
	Max	24 05	1 64	394 06	-5 03	1209 79	4 65	1118 50
225W	Mın	39 65	-1 25	495 84	-1 12	443 46	0 51	203 30
	Max	40 52	-0 39	156 31	-0 13	51 46	2 23	903 77

Values for Voltage 1st Harmonic

Power		Avg (V)	Sensor 1 % Error	Sensor 1 Abs Diff (mV)	Sensor 2 % Error	Sensor 2 Abs Diff (mV)	Sensor 3 % Error	Sensor 3 Abs Diff (mV)
75W	Min	10.118	-1.06	106.95	0.23	22.87	0.05	5.53
	Max	10.311	-0.50	51.57	0.75	77.83	0.53	54.19
150W	Min	16.028	-0.58	93.05	-0.83	132.57	0.72	115.81
	Max	16.204	-0.30	48.22	-0.28	45.20	1.41	228.09
225W	Min	3.575	-1.36	48.58	1.00	35.64	-0.19	6.88
	Max	3.620	-0.93	33.73	1.34	48.35	0.15	5.43

Values for Voltage 2nd Harmonic

Power		Avg (V)	Sensor 1 % Error	Sensor 1 Abs Diff (mV)	Sensor 2 % Error	Sensor 2 Abs Diff (mV)	Sensor 3 % Error	Sensor 3 Abs Diff (mV)
75W	Min	33.199	-0.78	257.90	-1.22	406.01	0.30	98.00
	Max	36.630	0.74	269.69	0.32	117.19	1.18	433.91
150W	Min	70.592	0.07	46.37	-1.23	865.11	0.27	193.14
	Max	71.974	0.37	265.29	-0.58	418.74	1.07	770.82
225W	Min	29.119	-1.33	388.59	1.56	455.36	-1.33	386.60
	Max	29.301	-0.82	240.28	2.15	629.31	-0.24	70.13

Values for Voltage 3rd Harmonic

Power		Avg (V)	Sensor 1 % Error	Sensor 1 Abs Diff (mV)	Sensor 2 % Error	Sensor 2 Abs Diff (mV)	Sensor 3 % Error	Sensor 3 Abs Diff (mV)
75W	Min	0.751	0.48	3.60	-8.06	60.54	-0.73	5.46
	Max	1.443	7.16	103.35	-0.04	0.58	3.47	50.11
150W	Min	3.583	-0.29	10.40	-0.66	23.63	-0.76	27.34
	Max	3.695	0.30	11.19	0.46	17.00	0.69	25.64
225W	Min	3.880	-1.28	49.64	1.14	44.19	-2.11	81.91
	Max	3.969	-0.25	9.85	2.36	93.66	-0.01	0.46

Values for Voltage 4th Harmonic

Power		Avg (V)	Sensor 1 % Error	Sensor 1 Abs Diff (mV)	Sensor 2 % Error	Sensor 2 Abs Diff (mV)	Sensor 3 % Error	Sensor 3 Abs Diff (mV)
75W	Min	0.647	-0.11	0.74	-6.63	42.87	-0.15	0.96
	Max	1.053	5.08	53.53	0.04	0.45	3.50	36.85
150W	Min	5.674	0.44	25.24	-4.45	252.65	1.93	109.38
	Max	5.914	1.17	69.48	-2.99	176.89	3.76	222.54
225W	Min	2.414	-1.20	28.87	1.08	26.12	-2.03	49.02
	Max	2.464	-0.18	4.55	2.22	54.58	-0.03	0.81

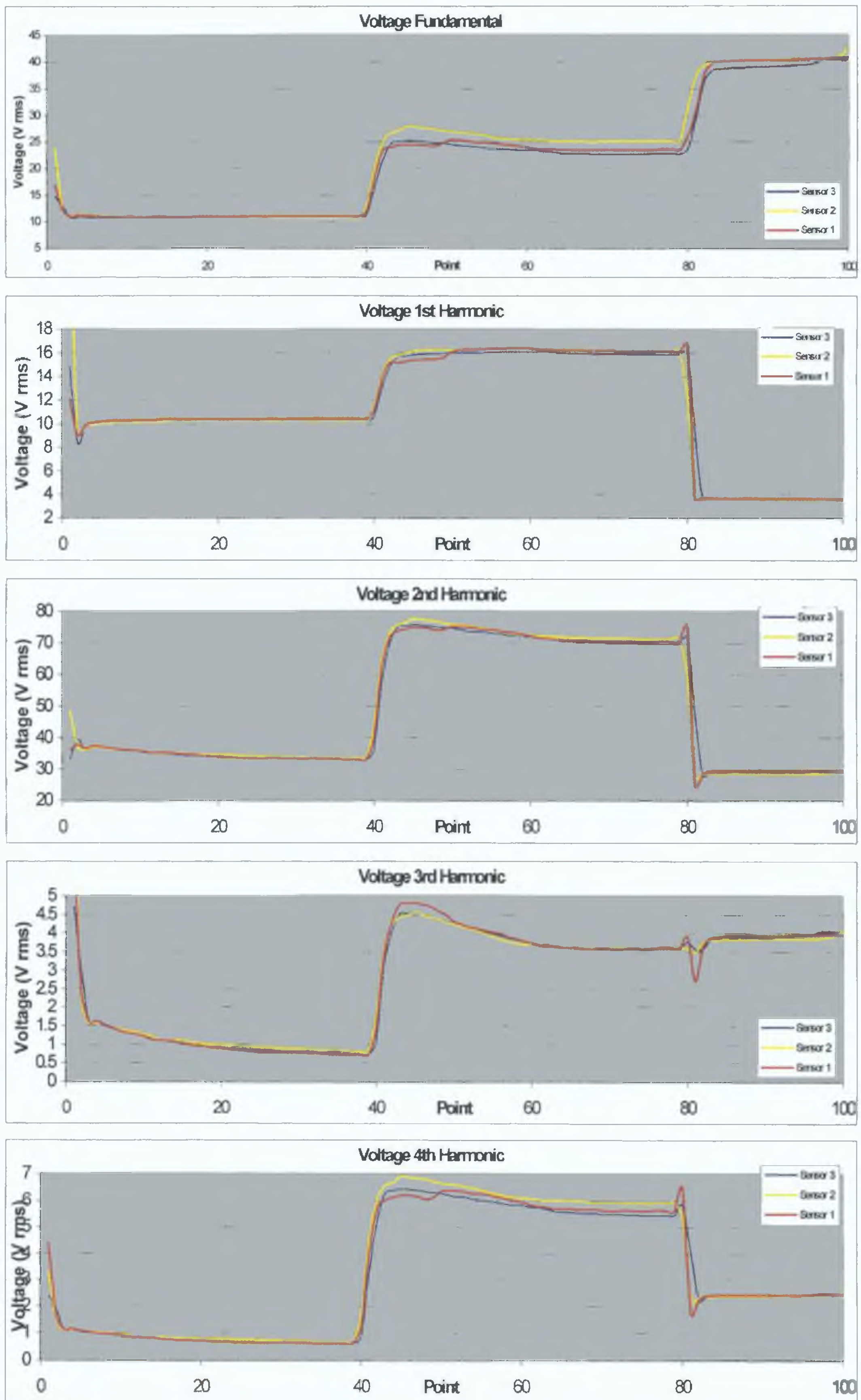

Figure 5.7 – Voltage Measurements for 3 Sensors

5.2 Current Measurement Repeatability

Again, as with the Voltage Fundamental measurements, very good repeatability can be seen with the Current Fundamental measurements The largest error is observed with the measurements of *Sensor 2*, and is approx 1 9%, corresponding to a real current difference of 177mA when the nominal current was 9 24A The smallest error is seen with *Sensor 3*, and is just 0 1% or 9 6mA on a nominal current of 9 24A

Values for Current Fundamental

Power		Avg (A)	Sensor 1 % Error	Sensor 1 Abs Diff (mA)	Sensor 2 % Error	Sensor 2 Abs Diff (mA)	Sensor 3 % Error	Sensor 3 Abs Diff (mA)
75W	Min	5 433	-1 54%	83 705	0 29%	15 542	0 46%	25 049
	Max	5 469	-0 97%	52 824	0 87%	47 632	0 87%	47 573
150W	Min	7 847	-1 25%	98 147	0 49%	38 429	0 53%	41 317
	Max	7 853	-1 10%	86 527	0 59%	46 680	0 75%	58 976
225W	Min	9 212	-1 88%	173 488	1 68%	154 528	-0 33%	30 565
	Max	9 242	-1 59%	146 561	1 92%	177 274	0 10%	9 612

Values for Current 1st Harmonic

Power		Avg (A)	Sensor 1 % Error	Sensor 1 Abs Diff (mA)	Sensor 2 % Error	Sensor 2 Abs Diff (mA)	Sensor 3 % Error	Sensor 3 Abs Diff (mA)
75W	Min	0 018	4 41%	0 773	-9 58%	1 679	-0 33%	0 058
	Max	0 021	9 08%	1 922	-5 44%	1 152	1 83%	0 388
150W	Min	0 117	1 38%	1 618	-7 30%	8 550	3 94%	4 609
	Max	0 122	1 97%	2 402	-5 70%	6 964	5 77%	7 052
225W	Min	0 008	1 18%	0 099	-1 83%	0 154	-2 24%	0 189
	Max	0 009	2 91%	0 248	-0 66%	0 056	-0 02%	0 002

Values for Current 2nd Harmonic

Power		Avg (A)	Sensor 1 % Error	Sensor 1 Abs Diff (mA)	Sensor 2 % Error	Sensor 2 Abs Diff (mA)	Sensor 3 % Error	Sensor 3 Abs Diff (mA)
75W	**Min**	0 116	-1 15%	1 334	-5 73%	6 650	5 00%	5 805
	Max	0 130	0 58%	0 758	-4 15%	5 383	5 95%	7 720
150W	**Min**	0 289	0 19%	0 544	-6 20%	17 905	4 84%	13 965
	Max	0 297	0 58%	1 731	-5 33%	15 796	5 90%	17 493
225W	**Min**	0 103	-1 79%	1 843	-2 65%	2 735	3 26%	3 362
	Max	0 104	-1 28%	1 328	-1 98%	2 063	4 43%	4 618

Values for Current 3rd Harmonic

Power		Avg (A)	Sensor 1 % Error	Sensor 1 Abs Diff (mA)	Sensor 2 % Error	Sensor 2 Abs Diff (mA)	Sensor 3 % Error	Sensor 3 Abs Diff (mA)
75W	**Min**	0 022	-2 63%	0 574	-5 99%	1 308	4 47%	0 976
	Max	0 028	1 08%	0 308	-2 37%	0 675	6 55%	1 866
150W	**Min**	0 137	-1 27%	1 738	-4 31%	5 899	3 73%	5 105
	Max	0 143	-0 65%	0 925	-2 93%	4 178	5 43%	7 755
225W	**Min**	0 026	-3 67%	0 941	0 97%	0 248	1 16%	0 298
	Max	0 026	-2 82%	0 729	1 69%	0 436	2 58%	0 666

Values for Current 4th Harmonic

Power		Avg (A)	Sensor 1 % Error	Sensor 1 Abs Diff (mA)	Sensor 2 % Error	Sensor 2 Abs Diff (mA)	Sensor 3 % Error	Sensor 3 Abs Diff (mA)
75W	**Min**	0 014	-4 08%	0 557	-0 62%	0 084	1 84%	0 251
	Max	0 014	-1 65%	0 233	1 00%	0 141	3 34%	0 472
150W	**Min**	0 036	-2 80%	1 006	1 81%	0 651	-0 43%	0 153
	Max	0 037	-2 19%	0 807	2 70%	0 997	0 67%	0 248
225W	**Min**	0 019	-4 05%	0 786	3 33%	0 646	-0 11%	0 021
	Max	0 020	-3 46%	0 681	3 65%	0 717	0 50%	0 099

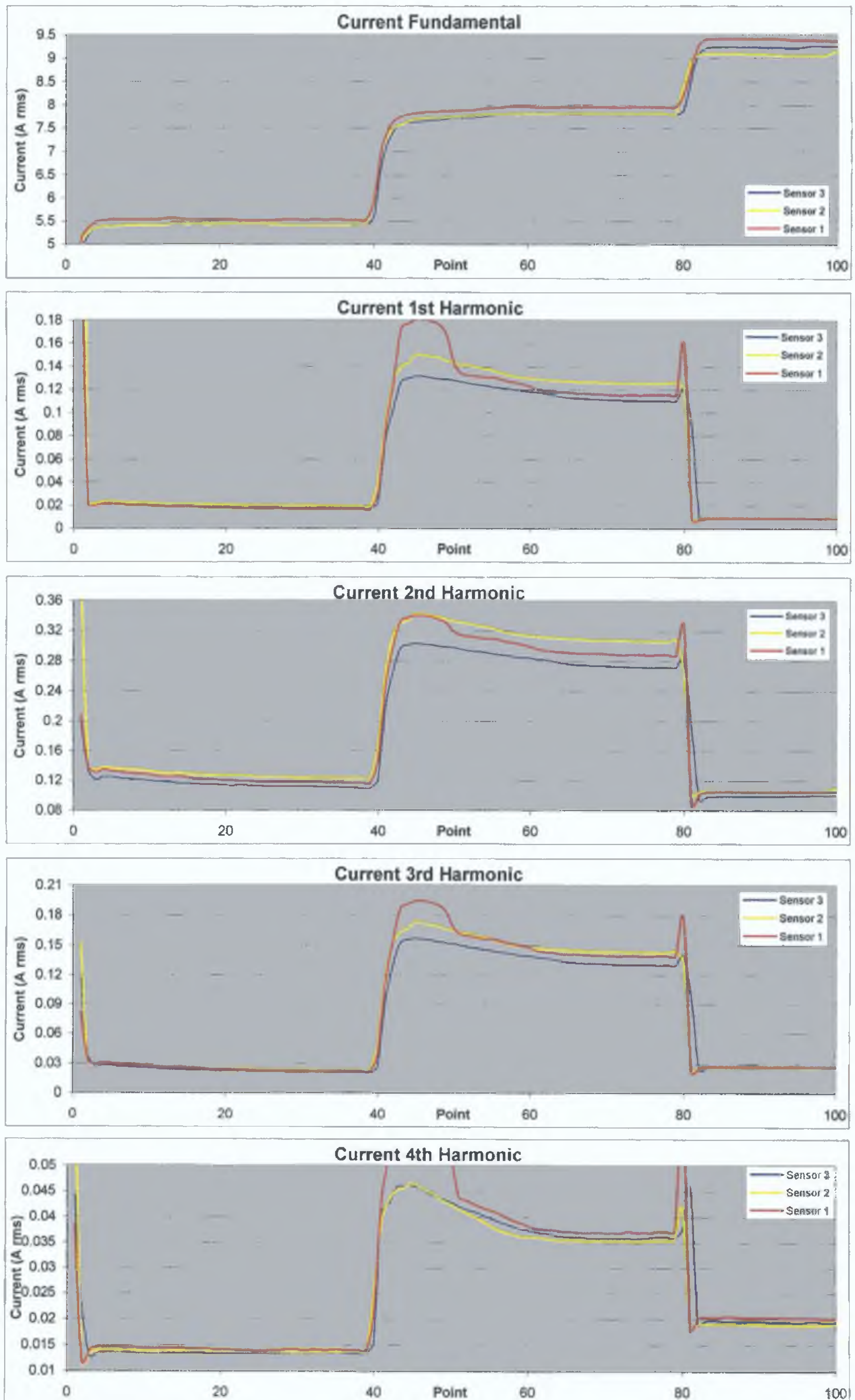

Figure 5.8 – Current Measurements for 3 Sensors

5.3 Phase Measurement Repeatabılıty

Good phase repeatabılıty and accuracy are very much ınfluenced by the qualıty of the ınstallatıon of the sensor, and ıts locatıon That ıs, ıf the sensor ıs located ın an envıronment where there are sıgnıficant RF fields or the groundıng of the top plate of the sensor ıs not good ın terms of an RF ground, the Phase measurement suffers as ıt ıs derıved from the Voltage and Current measurements

However, the measurements do show good repeatabılıty The smallest error ıs observed wıth *Sensor 1* (0 2° on a nomınal phase of –68 8°) and the largest error ıs also observed wıth *Sensor 2* (5 7° wıth a nomınal phase of –8 8°) Agaın note that from Fıgure 5 9, the measurements taken wıth *Sensor 2* durıng the first power step, where the phase ıs changıng from approx -15° to 0°, devıate from those taken wıth *Sensor 1* and *Sensor 3*

Values for Phase Fundamental

Power		Avg (Deg)	Sensor 1 Abs Dıff (Deg)	Sensor 2 Abs Dıff (Deg)	Sensor 3 Abs Dıff (Deg)
75W	Mın	-8 78	0 566	5 687	3 166
	Max	6 89	1 964	3 869	4 250
150W	Mın	-42 07	0 530	2 414	1 552
	Max	-41 74	0 715	2 246	1 848
225W	Mın	-68 79	0 196	0 582	0 203
	Max	-68 28	0 305	0 448	0 343

Values for Phase 1st Harmonıc

Power		Avg (Deg)	Sensor 1 Abs Dıff (Deg)	Sensor 2 Abs Dıff (Deg)	Sensor 3 Abs Dıff (Deg)
75W	Mın	-42 82	4 367	4 404	1 442
	Max	-41 53	3 608	5 633	0 657
150W	Mın	-39 99	1 329	2 033	1 102
	Max	-39 52	1 182	2 312	0 848
225W	Mın	-52 28	3 084	4 604	2 338
	Max	-51 04	2 266	4 907	1 794

Values for Phase 2nd Harmonic

Power		Avg (Deg)	Sensor 1 Abs Diff (Deg)	Sensor 2 Abs Diff (Deg)	Sensor 3 Abs Diff (Deg)
75W	Min	80 62	3 426	3 084	0 496
	Max	81 20	3 563	2 977	0 397
150W	Min	79 98	3 498	2 784	0 798
	Max	80 06	3 559	2 736	0 752
225W	Min	81 79	3 380	2 778	0 658
	Max	81 83	3 408	2 734	0 617

Values for Phase 3rd Harmonic

Power		Avg (Deg)	Sensor 1 Abs Diff (Deg)	Sensor 2 Abs Diff (Deg)	Sensor 3 Abs Diff (Deg)
75W	Min	92 54	1 891	3 566	0 052
	Max	99 30	2 840	1 998	1 213
150W	Min	149 72	2 334	0 141	2 665
	Max	150 10	2 729	0 102	2 380
225W	Min	97 33	2 241	2 690	0 203
	Max	98 30	2 557	2 343	0 342

Values for Phase 4th Harmonic

Power		Avg (Deg)	Sensor 1 Abs Diff (Deg)	Sensor 2 Abs Diff (Deg)	Sensor 3 Abs Diff (Deg)
75W	Min	-125 02	0 630	0 863	3 485
	Max	-109 80	1 880	2 727	2 066
150W	Min	-143 78	0 792	2 180	1 766
	Max	-143 40	0 494	2 428	1 482
225W	Min	134 41	1 757	2 239	0 173
	Max	135 45	2 076	1 903	0 322

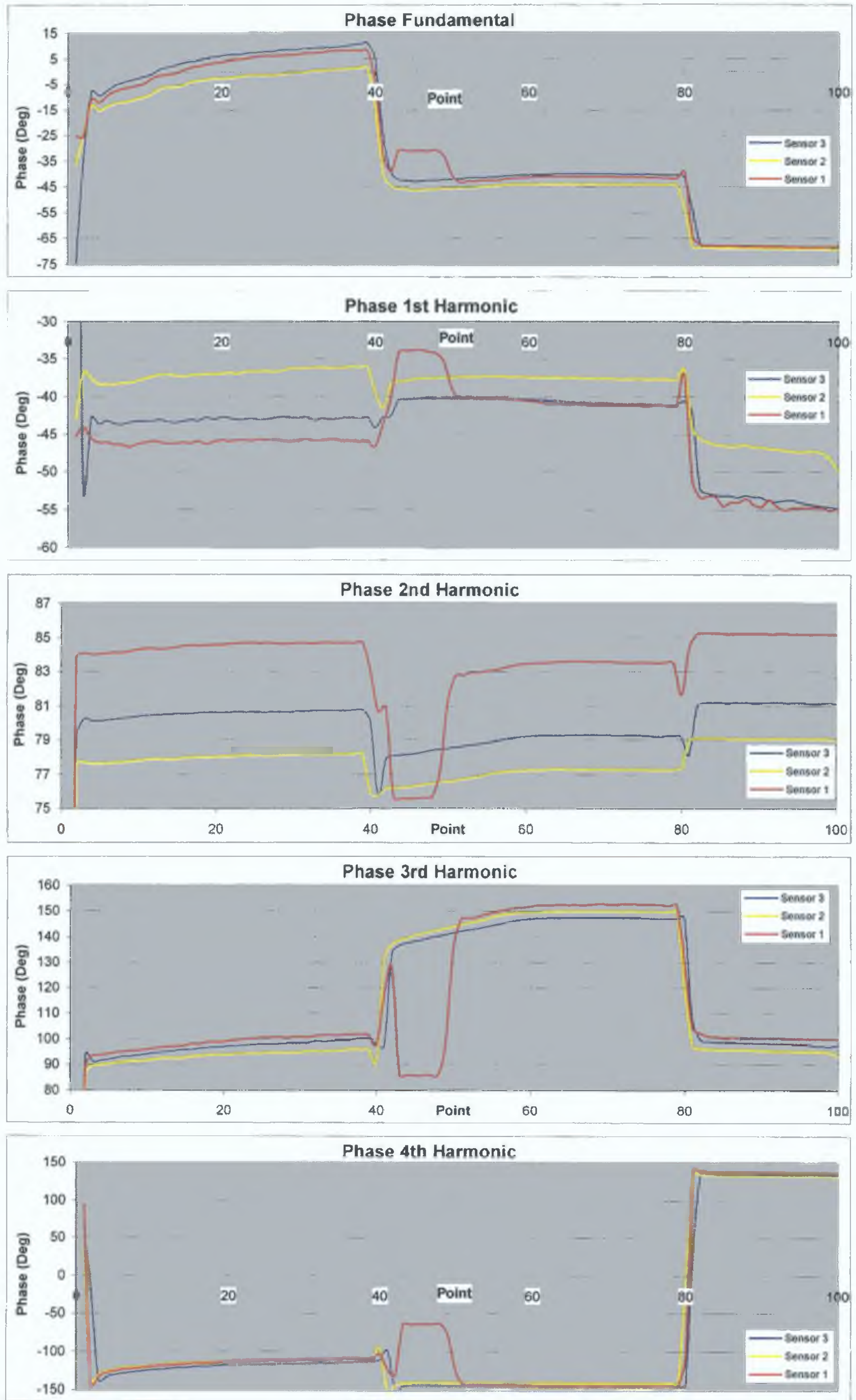

Figure 5.9 – Phase Measurements for 3 Sensors

5.4 Measurement Resolution

The PIM is a high resolution system due to the method of coherent sampling and signal averaging employed The table below highlights the measurement resolution (for fundamental values only) of the system using the data recorded from the *3 Sensor* experiment The resolution is calculated as a percentage of two subsequent measurements, according to the equation

$$\frac{M_2 - M_1}{Mean(M_1 + M_2)} \times 100\% \qquad (5\ 1)$$

where M_1 = first measurement
M_2 = second, subsequent measurement

Note The Phase resolution is calculated as a difference as this a more useful parameter for representing Phase resolution

Resolution of Sensor 1

Fundamental Voltage				
Power	**M_1**	**M_2**	**Abs Diff (mV)**	**Abs Diff (%)**
75W	10 85335	10 85346	0 11	0 0010%
150W	23 42547	23 42437	1 10	0 0047%
225W	40 49251	40 48890	3 61	0 0089%
Fundamental Current				
Power	**M_1**	**M_2**	**Abs Diff (mA)**	**Abs Diff (%)**
75W	5 51046	5 51024	0 214	0 0039%
150W	7 94006	7 94007	0 004	0 0001%
225W	9 35374	9 35369	0 053	0 0006%
Fundamental Phase				
Power	**M_1**	**M_2**	**Abs Diff (Deg)**	
75W	8 08136	8 04230	0 0390	
150W	-41 24897	-41 24741	0 0016	
225W	-68 03867	-68 03732	0 0014	

Resolution of Sensor 2

Fundamental Voltage

Power	M_1	M_2	Abs Diff (mV)	Abs Diff (%)
75W	10 70467	10 70397	0 70	0 0067%
150W	25 10377	25 10351	0 26	0 0010%
225W	42 83236	42 83621	3 85	-0 0090%

Fundamental Current

Power	M_1	M_2	Abs Diff (mA)	Abs Diff (%)
75W	5 40943	5 40945	0 02	0 0003%
150W	7 80764	7 80771	0 07	0 0009%
225W	9 08658	9 08660	0 03	0 0003%

Fundamental Phase

Power	M_1	M_2	Abs Diff (Deg)
75W	-2 82429	-2 84311	0 0188
150W	-44 16699	-44 16213	0 0049
225W	-68 87457	-68 87550	0 0009

Resolution of Sensor 3

Fundamental Voltage

Power	M_1	M_2	Abs Diff (mV)	Abs Diff (%)
75W	10 86950	10 86908	0 42	0 0039%
150W	22 60520	22 60702	1 82	0 0081%
225W	40 53396	40 53754	3 58	0 0088%

Fundamental Current

Power	M_1	M_2	Abs Diff (mA)	Abs Diff (%)
75W	5 41181	5 41188	0 07	0 0012%
150W	7 78799	7 78785	0 14	0 0018%
225W	9 23948	9 23944	0 04	0 0004%

Fundamental Phase

Power	M_1	M_2	Abs Diff (Deg)
75W	6 64538	6 65834	0 0130
150W	-39 97995	-39 98192	0 0020
225W	-68 62762	-68 62940	0 0018

Chapter 6

PLASMA DIAGNOSTICS AND PIM APPLICATIONS

In the absence of thermodynamic equilibrium, the state of the plasma is determined by external parameters such as electrical power, pressure, gas flow rate, and internal parameters such as the rate constants of reactions Plasma technology has reached the stage where it is possible to control empirically the right combination of parameters to obtain highly reproducible results in the same or similar system Changes in these macroscopic variables will generally change the basic plasma conditions, but the precise manner of these changes is, in most cases, unknown

6.1 Plasma Diagnostics

The objective of plasma diagnostics is to obtain information about the state of the plasma by examination of the physical processes occurring in it or controlling it Plasma diagnostics can be classified into ex-situ and in-situ techniques Ex-situ, or off-line techniques, sample the contents of the plasma and transfer the sample outside the chamber for examination In-situ, or on-line techniques, provide real-time measurement of at least one plasma or process parameter A brief outline of the most used techniques for plasma diagnostics is given below

Mass Spectrometry

- Identifies molecules, radicals, atoms, or ions by their molecular or atomic weight
- Used for quantifying plasma composition or for process control
- Types available are Magnetic Analyser, Time-of-Flight Spectrometer, and Quadrupole Mass Spectrometer (QMS)
- QMS is most used type and analyses ions on the basis of their mass to charge ratio (*m/e*)
- Can be use for end-point detection in plasma etching
- Ex-situ, intrusive technique (considered intrusive because the sampling port is in direct contact with the plasma)

Electrostatic Probes

- Allows the determination of plasma density (n), electron temperature (T_e), plasma potential (V_p), and floating potential (V_f)
- Analysis of the probe IV characteristic yields the plasma parameters
- Most used types are single or double Langmuir probes
- In-situ, intrusive technique

Optical Methods

- Uses photons to transmit information from the plasma to the detection tool
- Techniques based on analysis of optical radiation and absorption by the plasma
- Provides information about the concentration of plasma species and their temperature
- Techniques include Optical Emission Spectroscopy (OES), Absorption Spectroscopy, Laser Induced Fluorescence, Raman Spectroscopy, Laser Interferometry
- OES can be used for process control in etch and deposition processes
- In-situ, non-intrusive technique

6 1 1 Impedance Probes

Process engineers generally understand the effects of traditional process variables such as gas flow rate, pressure, substrate temperature and bias However, measurement of the electrical RF parameters of plasmas and process chambers is being recognised as a very interesting diagnostic for plasma research and has shown great potential for semiconductor manufacturing [18,19,24,25] IV probes can be used to predict and diagnose machine faults and to monitor and control etch and deposition processes [18,24,25,29,32] For example, etch rate and etch uniformity are often used as tool-performance indicators [29] and the performance of the device manufactured can be affected by the performance of the etch process [13,31]

Including an IV sensor between the matching network and plasma chamber allows new electrical variables to be monitored and controlled [24,31,32] This can give engineers valuable assistance in diagnosing process variations Problems such as poor RF connections and faulty matching boxes [24,29], process changes due to changes in RF power, gas pressure and gas flow rates [18,24,25,31] can all be detected and solved

more easily by using RF impedance probes RF probes are an in-situ diagnostic that do not require complex set-up and calibration and can lead to improved wafer yield and overall equipment effectiveness The following sections discuss some applications of the PIM system

6 2 PIM Applications

The most important parameters that generally control or affect materials processing by plasmas are the following [18,24,31,32]

- Electrical power and frequency
- Partial pressures of feed gases and their flow rates
- Total reactor pressure
- Substrate temperature and bias
- Reactor geometry and material
- Chamber wall and electrode condition

These parameters have to be carefully controlled to define the plasma and achieve the desired process results For example, the RF power determines the plasma current and voltage The gas mixture composition can affect the chemical reactions inside the plasma reactor and the properties of the final product The combination of the gas feed, reactor pressure, and electrical power will each affect the rates of the reactions The reactor geometry and substrate temperature and bias can also affect the reaction rates A variation of the frequency can affect the number and energy of the ions that can follow the alternating field thus changing the flux and energy of the particles bombarding the plasma treated surface

By choosing a suitable reactor and adjusting the plasma parameters, it is possible to control the interaction between the physical and chemical mechanisms that determine the plasma to achieve the required process characteristics In future, it may be possible to model the plasma and predict the outcome of each process step [26], and even to generate an alarm or shut down the tool when the process drift, if allowed to continue, would result in product damage [27]

6 2 1 RF Power Delivery and Match Unit Variations

The only aspect of the RF power that has historically been monitored has been the power transferred between the RF generator and the matching network, namely the forward and reflected powers Matching network losses are generally unaccounted for and can be quite high and variable [18,25,31] Therefore, it may be difficult to know the actual power delivered to the plasma, and hence, its effect on the process

Traditionally, the RF setpoint for a plasma process is the generator output power and it is this power that is controlled during the process period However, the power measured is the power that is delivered to the matching network and plasma, and does not indicate the plasma power alone Power losses that occur in the matching network and the RF delivery path can be considerable and it is, therefore, not possible to determine how much of the generator power is actually consumed by the plasma [18,29,31] In addition, hardware differences from tool to tool may also effect the power transfer efficiency and result in variations in the process performance for the same nominal process conditions [18,19,25,31]

By installing an IV sensor after matching networks, post-match measurement can be performed with this information being used for feedback control of the generator or match network [18] It may even be possible to use the sensor for diagnostics of the complete tool hardware [24,29] For example, Figure 6 2 shows the Voltage and Current measurements taken by a PIM system that was installed on an Applied Materials DPS poly-silicon etch tool [40]

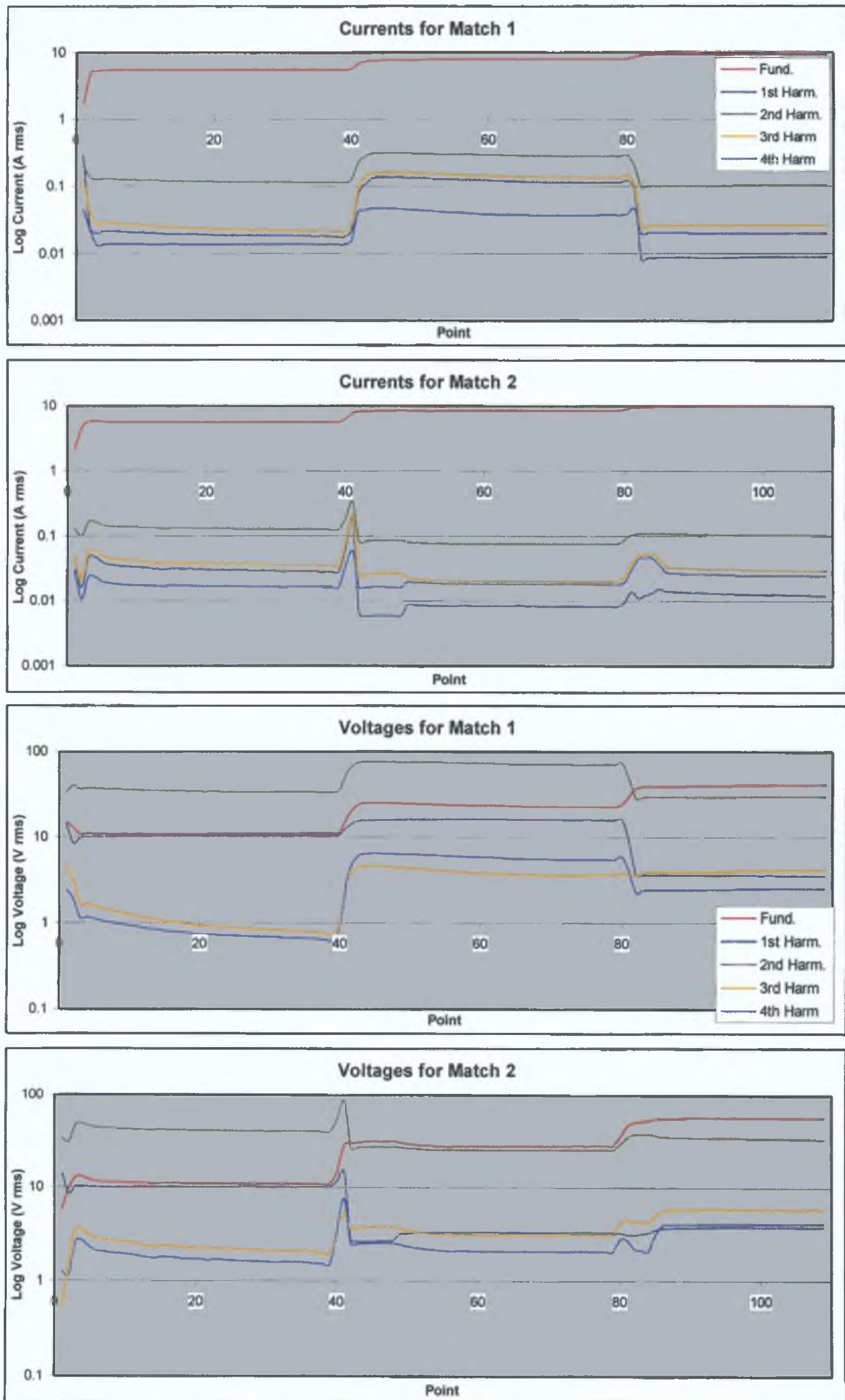

Fig. 6.2 – RF Voltage and Current for Two Matching Units

During this experiment, the matching network used with the tool was replaced by an identical type and the same process steps performed During the process, the power is increased in three steps, as can be seen by the increase in the Fundamental Voltage and Current measurements However, the performance of the second matching network is considerably different from that of the first at the harmonics The harmonics of the second match do not increase as they do for the first match In addition, the Second harmonic of the Voltage for the first match is significantly larger than the Fundamental This is to be expected for an ICP reactor, but is not observed when the second match is installed

Matching networks maximise the generator output power delivered to the plasma by transforming the complex load of the plasma so that it appears as a purely 50Ω resistive load This does not, however, guarantee that the efficiency of the power transfer is 100% The efficiency, η, is given by [18,25]

$$\eta = \frac{R_L}{R_L + R_M} \tag{6 1}$$

where R_L = load resistance
R_M = match resistance

Therefore, the efficiency only approaches 100% when $R_L \gg R_M$ The efficiency depends on the load resistance, which in turn, depends on the plasma, and hence process conditions However, any differences in the match resistance will lead directly to differences in the power delivered In addition, variations in the stray capacitance of the RF circuit can reduce the overall efficiency of RF power delivery by dissipating more power in the matching network Therefore, changes in the process, matching network resistance and stray capacitance can produce variations in tool to tool performance [18,25]

Patrick et al [18] have shown, using a LAM Research TCP 9400PTX silicon etching system, that there is a 5% increase in etch rate when one match is compared to another They have also shown that the etch rate decreases if the stray capacitance (from chuck to ground) is increased These factors have been attributed to the poor match efficiency

6 2 2 Chamber Clean End Point

Rather than just measure the power dissipated in the plasma, the PIM measures the plasma Voltage, Current and Phase angle between the voltage and current It performs these measurements for the fundamental and first four harmonics A process change may not be seen by simply observing the power but will be indicated by changes in either the voltage, current or phase [18,24,25] In addition, once the basic RF parameters have been measured, the plasma impedance can be determined

The plasma impedance is a complex quantity, with resistive, inductive and capacitive components A change in any one component can affect the plasma process and hence, the quality of the product being processed By accurately measuring the plasma RF parameters, changes in the load impedance can be compensated for In fact, any change in the plasma process such as gas pressure and mixture, RF power, chamber condition, and wafer condition will each affect the measured RF parameters [17,18,24,25,31,32]

Figure 6 3 shows the variation of the plasma impedance during a Silicon Nitride chamber clean process measured by a PIM system installed on a commercial process tool Observe how the 3rd Harmonic of the Impedance abruptly changes as the end point of the chamber clean is reached A similar change in the 2nd Harmonic is also observed, but is less severe The end point was determined using a conventional optical method

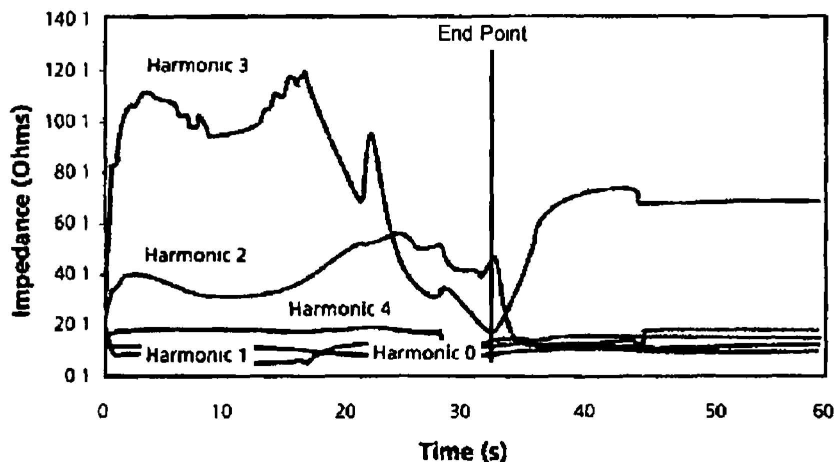

Fig. 6 3 – Plasma Impedance Variation during Chamber Clean

6 2 3 Etch End Point

Plasma etching is a complex process to control [13,29], and can account for almost one-third of the total number of wafers scrapped during present day semiconductor fabrication [29] As the endpoint of the etch process is reached, the chemical composition of the plasma changes as the area of the etched material decreases [18] This can cause the underlying film to be damaged if the process is not stopped in time As device complexity continues to push plasma etch tools toward the limit of their capabilities, understanding all the sources of variability that can exist in the etch process becomes imperative

Monitoring the plasma RF current and voltage can provide valuable data that can be used to detect etch endpoint [18,41] Several RF parameters undergo parallel changes at an etch endpoint stage and this information can be used to determine proper process termination Problems associated with optical endpoint detection, such as optical window clouding, detector drift and optical set-up, can then be avoided

Figure 6 4 shows the end point of an oxygen photoresist etch process being detected by a PIM system installed on a commercial etch tool The optical endpoint occurred at approx 140secs and can be seen to correspond to a dramatic change in the impedance of the 5th Harmonic of the Impedance

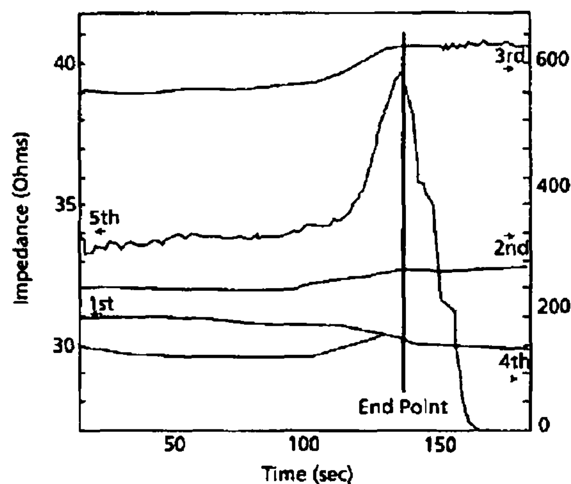

Fig 6 4 – Etch Endpoint Detection

6.3 Other Possible Applications

As the manufacture of semiconductor devices becomes more complex, tighter control of the processes and process equipment is required In addition, it is becoming critical to better understand the properties and effects of the plasma when processing different materials Plasma impedance sensors, such as the PIM, can perform this important role as they are non-intrusive, provide the accuracy and resolution required, and measure and report the data in real time

A summary of possible applications of impedance sensors is given below

- Power Levelling – the plasma process is a function of plasma power and not generator output power IV sensors can be used to accurately measure plasma power
- Etch Endpoint – a change in the gas composition due to the endpoint stage results in a plasma density change and corresponding plasma impedance shift
- Clean Endpoint – removal of polymer coatings on the chamber walls results in a plasma impedance change
- Chamber Matching – chamber condition after a preventative maintenance cycle can be checked by running a simple plasma and comparing known RF parameters
- Chamber Fingerprinting – by characterising the chamber in response to changes in a specific input parameter (e g power, pressure, flow rates), changes during a process run can be diagnosed
- RF Supply and Grounding – problems associated with chamber RF grounds, RF generators, match networks or RF delivery paths can be checked by measuring the RF parameters at known conditions
- Process Control and Fault Detection – variations in the conventional control parameters can be detected by using IV sensors, and the detection of malfunctions can reduce defective manufacturing

Chapter 7

CONCLUSION

An instrument capable of measuring the amplitude and phase of the first five Fourier components of the plasma Voltage and Current of RF plasma processing systems has been designed, tested and applied in real world applications The complete system design, including the technique of Coherent sampling that has enabled the superior measurement performance has been described as has the novel sensor design, which addresses some of the design flaws of conventional IV sensor design

The *Plasma Impedance Monitor* is capable of improving our understanding of plasmas by verifying current plasma equivalent models and may become as universally accepted as Langmuir probe measurements are today

It may also become an invaluable process control sensor for the semiconductor manufacturing process, or for any process where accurate control of RF plasmas are required It has been shown here and by others that knowledge of RF power generation, impedance matching and the RF delivery path to process chambers is not a simple matter It requires careful consideration and design if accurate device manufacture and high yield are required from an RF plasma process

It seems astounding that present day semiconductor manufacture is now capable of producing devices with feature sizes smaller than 0 18μm but that the only location where the RF power is controlled is where the RF generator and the matching network connect It has been shown that power losses in matching networks are high and may vary during the period of the process The RF power is the energy source that sustains the plasma, and it is the plasma that is the mechanism by which the process of etching or deposition proceeds It would seem, therefore, that accurate control of the RF power delivered to the plasma be imperative to obtaining satisfactory process results

The design of the *PIM* can be customised to suit a particular process or chamber, providing the level of control and functionality required It may even be possible to use *Artificial Intelligence* or *Expert Systems* with plasma or process models to predict the outcome of the process and control the tool accordingly

APPENDIX A

The following pages contain the circuit schematic diagrams of the *RF Vector Integrator*, and are detailed as follows

Sheet 1 Hierarchical view of the circuit sections

Sheet 2 Input termination and Programmable Gain Amplifiers

Sheet 3 Analogue to Digital Converters and Voltage References

Sheet 4 Clock Signal Auto Gain Amplifier and Comparator

Sheet 5 Sampling Frequency Generator (PLL) and Multiplier

Sheet 6 Logic Array IC for Registers

Sheet 7 Logic Array IC for PC Interface

Sheet 8 Logic Array IC for Acquisition and Look Up Table RAM

Sheet 9 RAM Feedback Registers

Sheet 10 Logic Array IC's for 24-Bit Accumulators

Sheet 11 Voltage Signal RAM

Sheet 12 Current Signal RAM

Sheet 13 External Digital Input

Sheet 14 Analogue Voltage Supply Generation and Decoupling

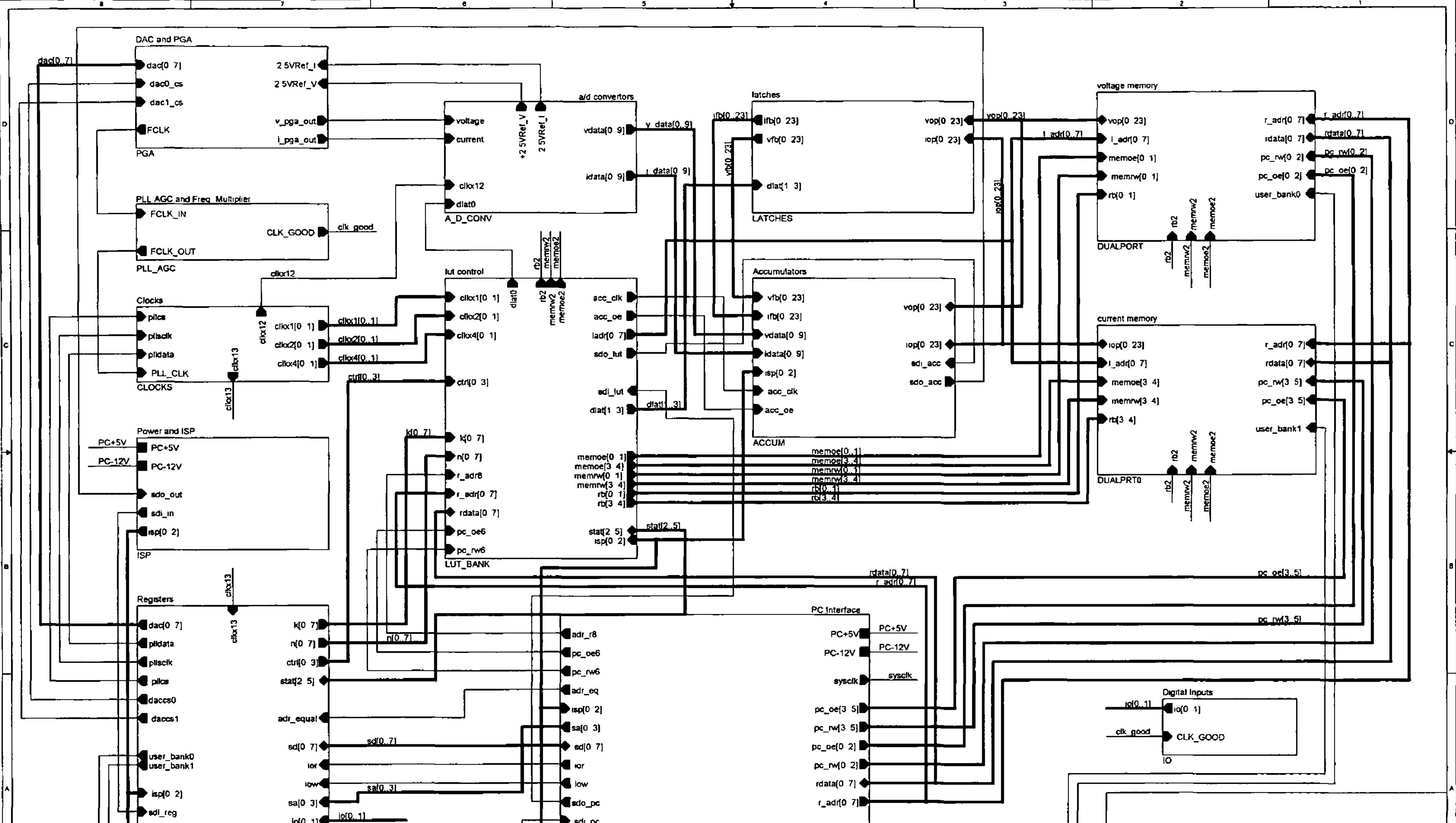
DAC and PGA
dac[0 7]
dac0_cs
dac1_cs
FCLK
2 5VRef_I
2 5VRef_V
v_pga_out
i_pga_out
PGA
PLL AGC and Freq Multiplier
FCLK_IN
CLK_GOOD
clk_good
FCLK_OUT
PLL_AGC
Clocks
pllcs
pllsclk
plldata
PLL_CLK
clkx1[0 1]
clkx2[0 1]
clkx4[0 1]
clkx12
clkx13
CLOCKS
Power and ISP
PC+5V
PC-12V
sdo_out
sdi_in
isp[0 2]
ISP
Registers
dac[0 7]
plldata
pllsclk
pllcs
daccs0
daccs1
user_bank0
user_bank1
isp[0 2]
sdi_reg
sdo_reg
k[0 7]
n[0 7]
ctrl[0 3]
stat[2 5]
adr_equal
sd[0 7]
ior
iow
sa[0 3]
io[0 1]
sysclk
REG
a/d convertors
voltage
current
clkx12
dlat0
+2 5VRef_V
2 5VRef_I
vdata[0 9]
idata[0 9]
v_data[0 9]
i_data[0 9]
A_D_CONV
lut control
clkx1[0 1]
clkx2[0 1]
clkx4[0 1]
ctrl[0 3]
k[0 7]
n[0 7]
r_adr8
r_adr[0 7]
rdata[0 7]
pc_oe6
pc_rw6
acc_clk
acc_oe
iadr[0 7]
sdo_lut
sdi_lut
dlat[1 3]
memoe[0 1]
memoe[3 4]
memrw[0 1]
memrw[3 4]
rb[0 1]
rb[3 4]
stat[2 5]
isp[0 2]
rb2
memrw2
memoe2
LUT_BANK
latches
ifb[0 23]
vfb[0 23]
dlat[1 3]
vop[0 23]
iop[0 23]
LATCHES
Accumulators
vfb[0 23]
ifb[0 23]
vdata[0 9]
idata[0 9]
isp[0 2]
acc_clk
acc_oe
vop[0 23]
iop[0 23]
sdi_acc
sdo_acc
ACCUM
voltage memory
vop[0 23]
i_adr[0 7]
memoe[0 1]
memrw[0 1]
rb[0 1]
r_adr[0 7]
rdata[0 7]
pc_rw[0 2]
pc_oe[0 2]
user_bank0
DUALPORT
current memory
iop[0 23]
i_adr[0 7]
memoe[3 4]
memrw[3 4]
rb[3 4]
r_adr[0 7]
rdata[0 7]
pc_rw[3 5]
pc_oe[3 5]
user_bank1
DUALPRT0
PC Interface
adr_r8
pc_oe6
pc_rw6
adr_eq
isp[0 2]
sa[0 3]
sd[0 7]
ior
iow
sdo_pc
sdi_pc
PC+5V
PC-12V
sysclk
pc_oe[3 5]
pc_rw[3 5]
pc_oe[0 2]
pc_rw[0 2]
rdata[0 7]
r_adr[0 7]
PC_INT
Digital Inputs
io[0 1]
CLK_GOOD
IO
Title
Plasma Impedance Monitor PC Card Root Schematic Sheet
Size
B
Document Number
Rev
3 0
Date
Wednesday, October 27, 1999
Sheet 1 of 14

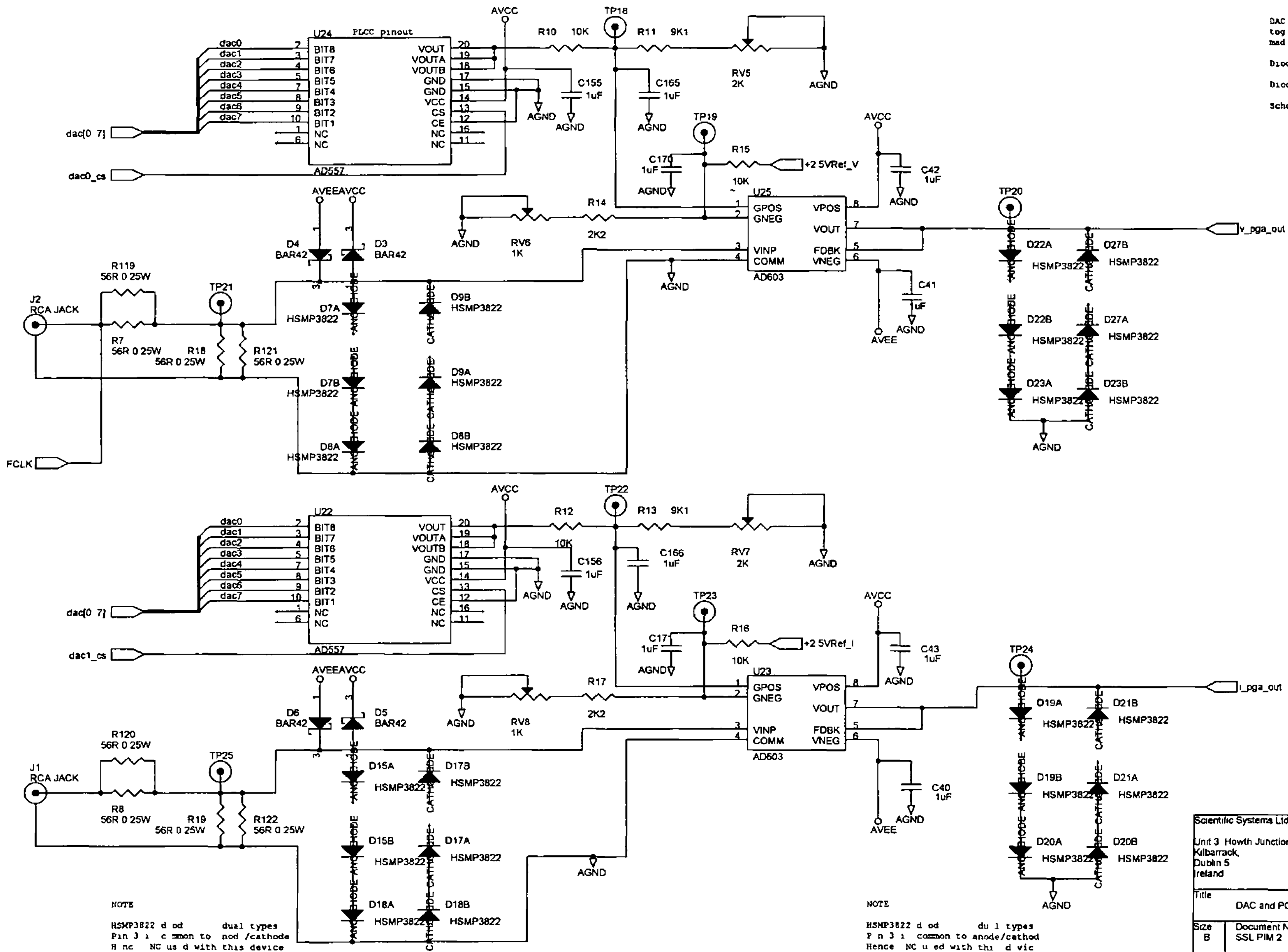

DAC Ground C nn ct DAC analog and digital g ound
tog th r t d v c If single ground conn ct o
mad u nalog ground

Diodes and Schottkys a e SOT23

Diodes r RF p t

Schottky diodes are ult a fas

Scientific Systems Ltd

Unit 3 Howth Junction Bus Park
Kilbarrack,
Dublin 5
Ireland

Title	DAC and PGA Circuit	
Size B	Document Number SSL PIM 2	Rev 3 0
Date	Monday, September 18, 2000	Sheet 2 of 14

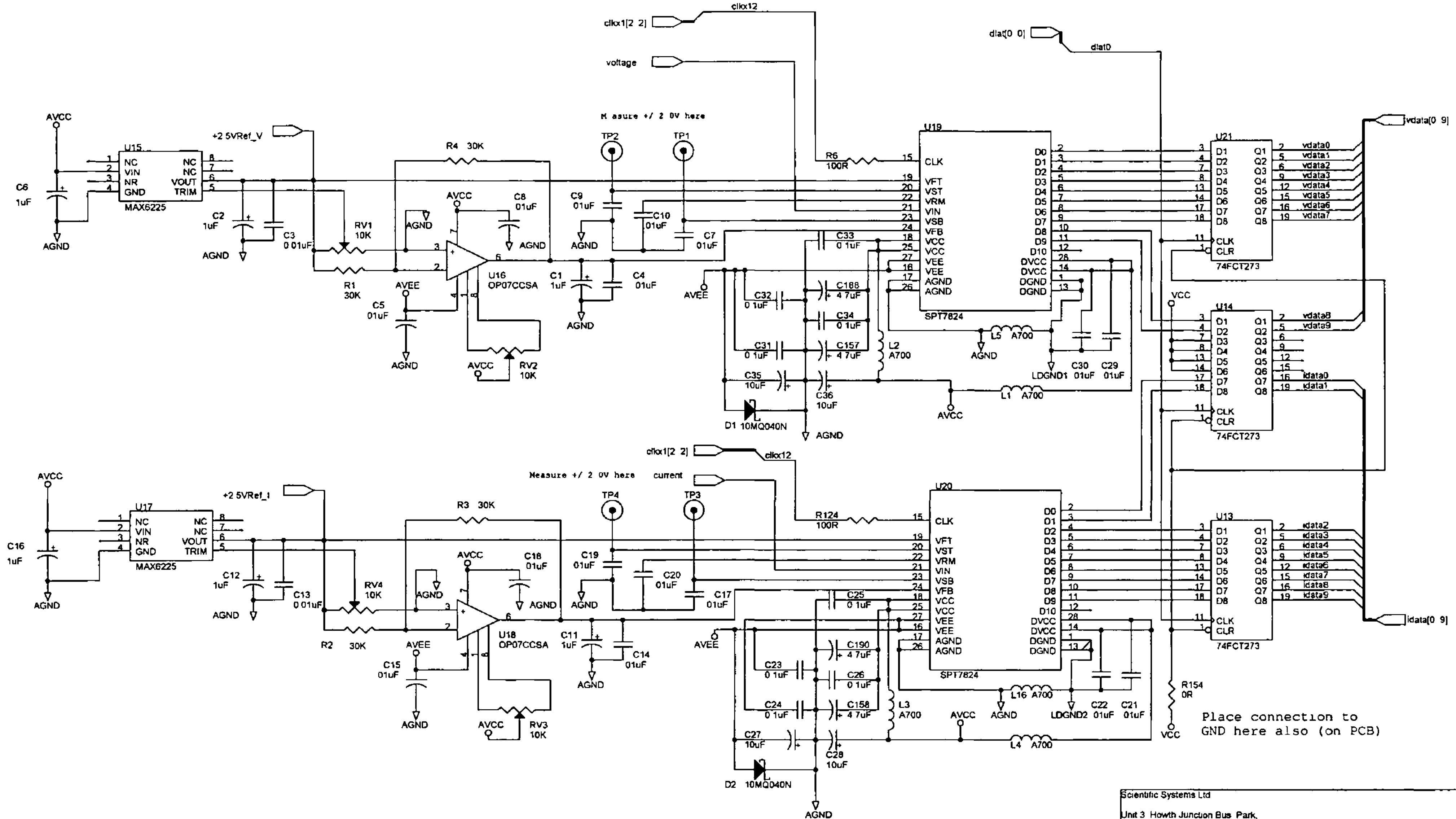

Scientific Systems Ltd

Unit 3 Howth Junction Bus Park,
Kilbarrack,
Dublin 5
Ireland

Title	Analog to Digital Convertors	
Size B	Document Number SSL PIM 4	Rev 3 0
Date	Wednesday, May 05, 1999	Sheet 3 of 14

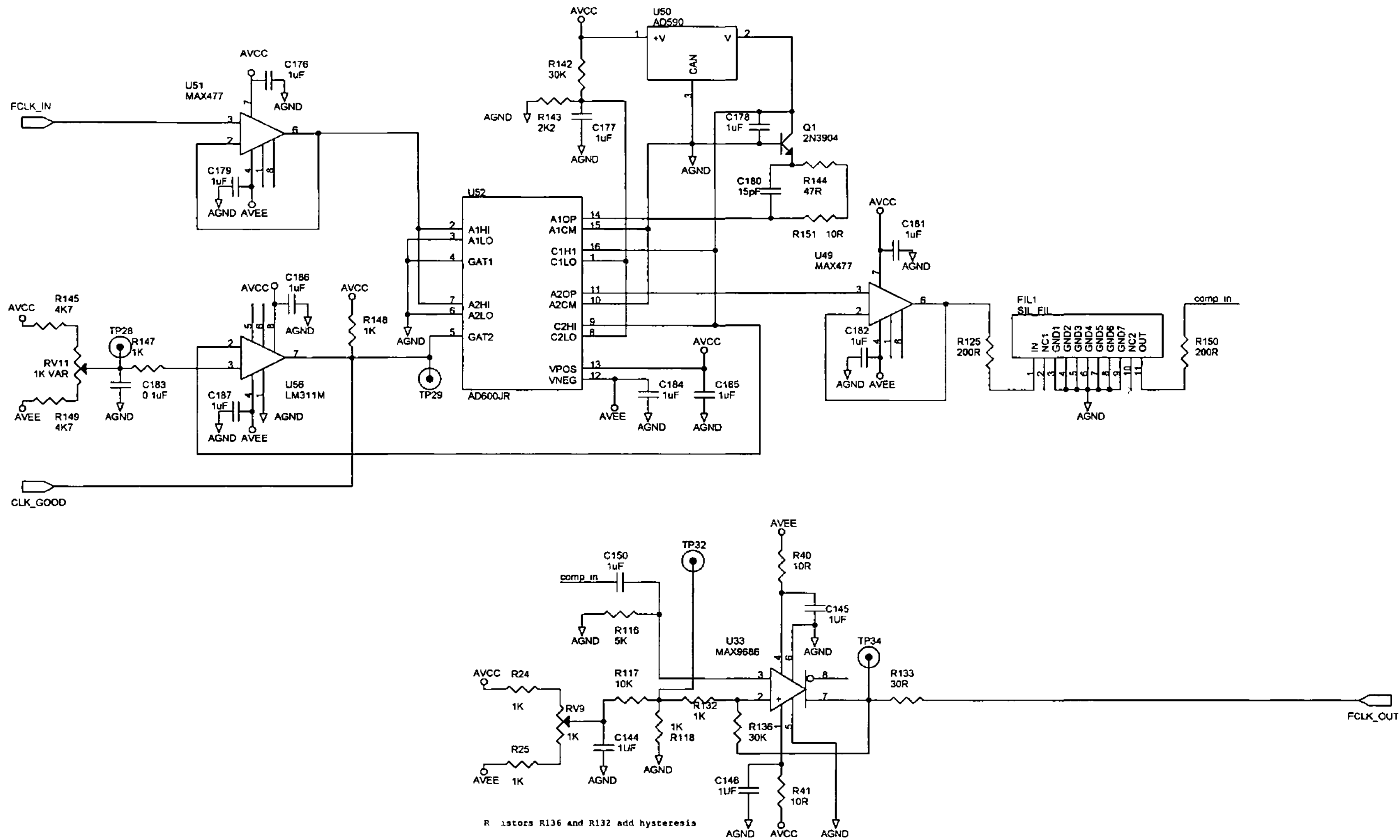

R istors R136 and R132 add hysteresis

The MAX9686 hould be plac as close as possible to the ingl join b twe n the analog and digital powe and g ound joins

Scientific Systems Ltd
Unit 3 Howth Junction Bus Park,
Kilbarrack,
Dublin 5
Ireland

Title	Clock Signal AGC and Freq Multiplier Circuit	
Size B	Document Number SSL PIM 14	Rev 3 0
Date	Monday, September 18, 2000	Sheet 4 of 14

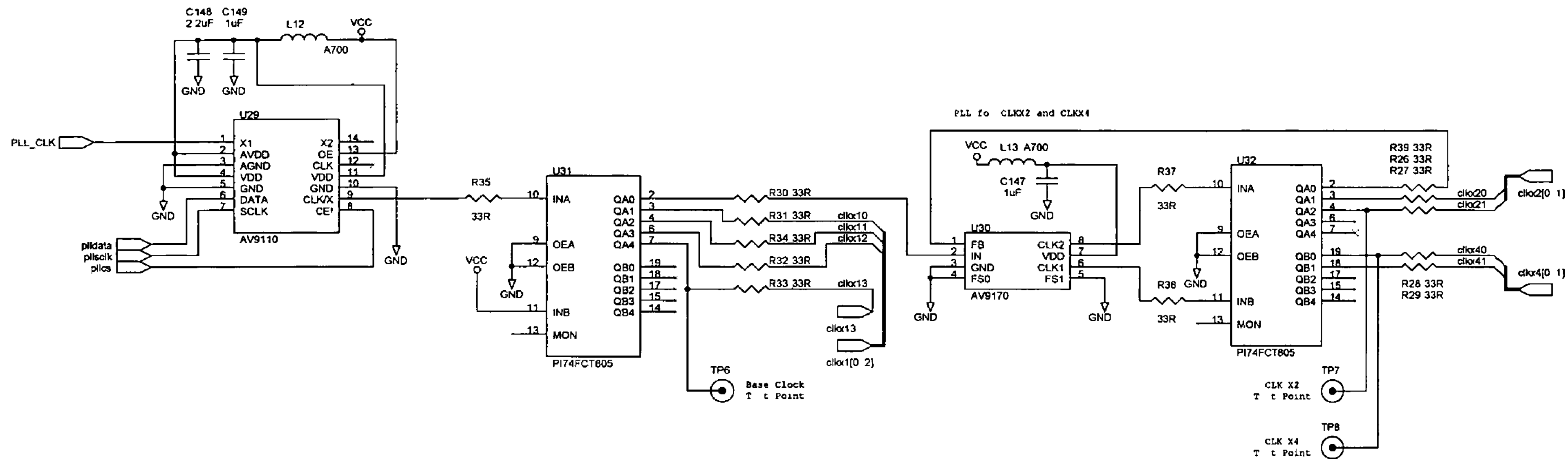

Scientific Systems Ltd Unit 3 Howth Junction Bus Park Kilbarrack, Dublin 5 Ireland		
Title	Clock Generator Circuit	
Size B	Document Number SSL PIM 3	Rev 3 0
Date	Monday, September 18, 2000	Sheet 5 of 14

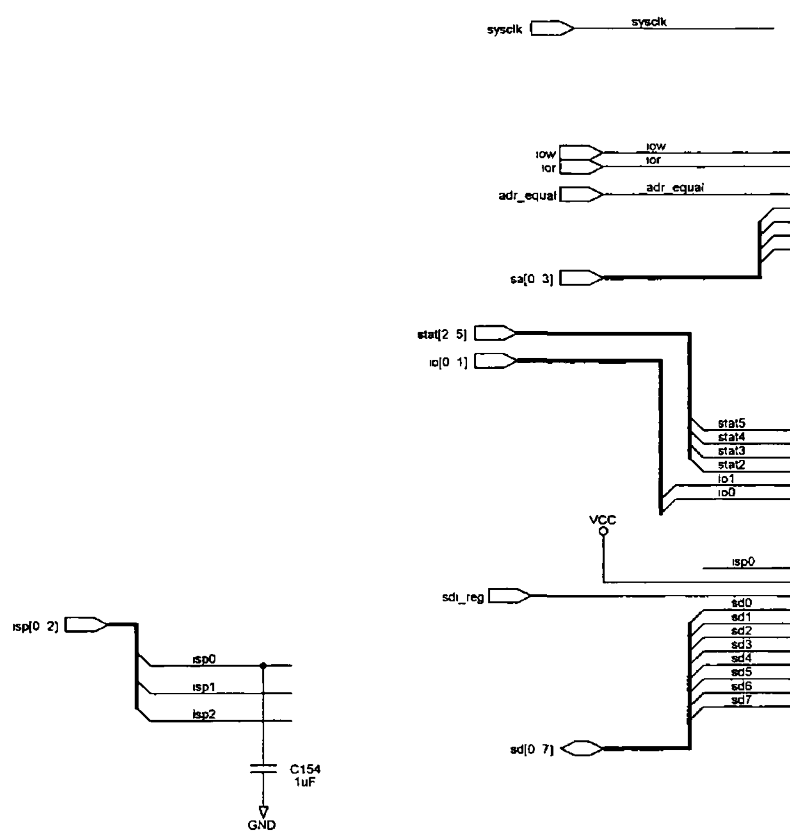

U46
ISPLSI1032
U47A
74F125
U47B
74F125
R111
R112
R113
33R
C154
1uF
GND
VCC
sysclk
iow
ior
adr_equal
sa[0 3]
stat[2 5]
io[0 1]
sdi_reg
sd[0 7]
isp[0 2]
daccs1
daccs0
plldata
pllsclk
pllcs
dac[0 7]
user_bank[0 1]
user_bank0
user_bank1
clkx13
ctrl6
ctrl[0 3]
k[0 7]
sdo_reg
n[0 7]
For test purposes n[0 7] and k[0 7] can b xamin d by
scope a th y do not ch ng dynamically
Two LSB DAC input te t point d only t t t timing
othe bits by scop
E amin
Scientific Systems Ltd
Unit 3 Howth Junction Bus Park,
Kilbarrack,
Dublin 5
Ireland
Title
Register PLD Schematic
Size
B
Document Number
SSL PIM 11
Rev
3 0
Date
Monday, September 18, 2000
Sheet 6 of 14

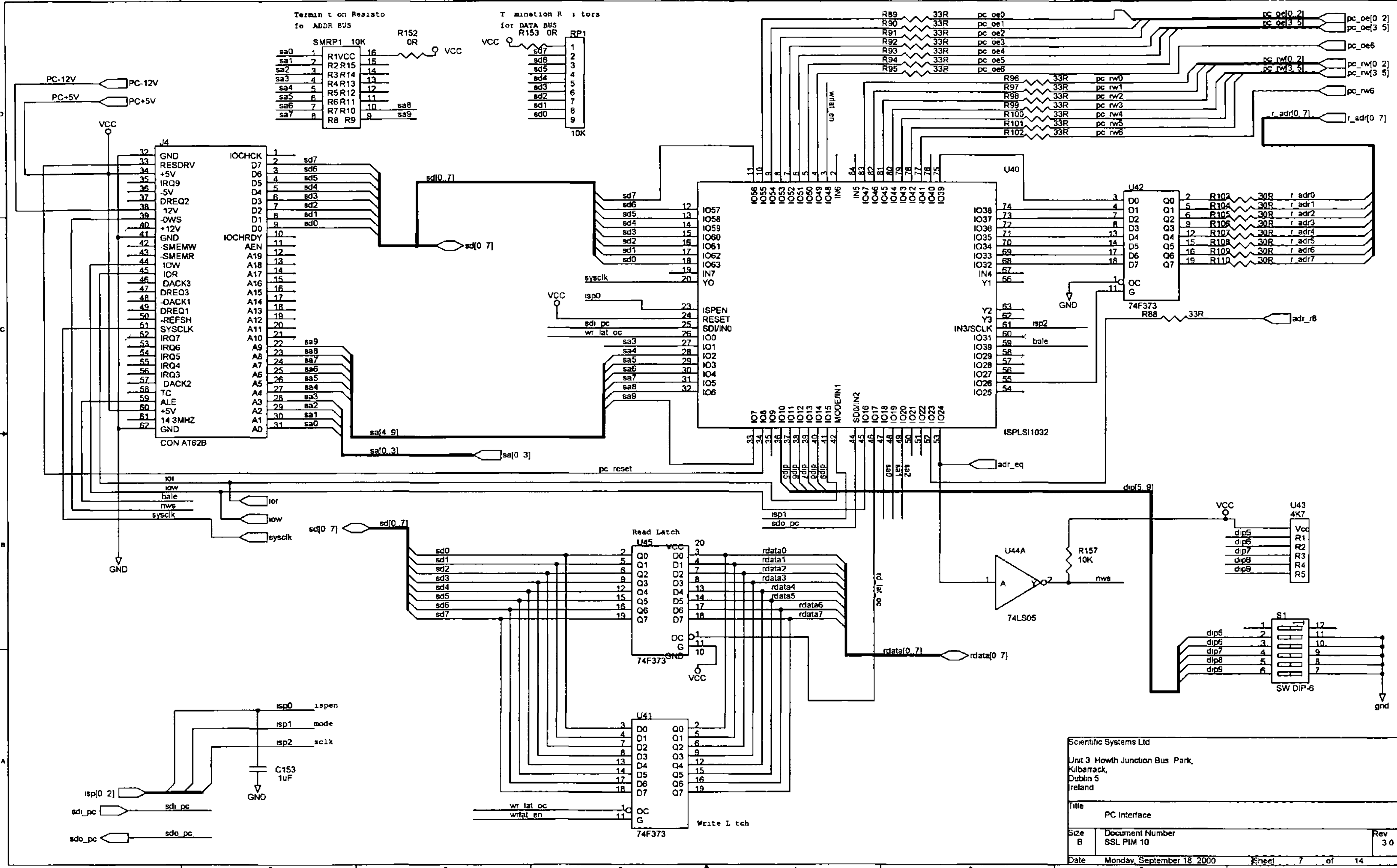

Termination Resistors for ADDR BUS
SMRP1 10K
R152 0R
Termination Resistors for DATA BUS
R153 0R
RP1
10K
J4
CON AT62B
U40
ISPLSI1032
U42
74F373
R88 33R
Read Latch
U45
74F373
U41
74F373
Write Latch
U44A
74LS05
R157 10K
U43 4K7
S1
SW DIP-6
C153 1uF
pc_oe[0 2]
pc_oe[3 5]
pc_oe6
pc_rw[0 2]
pc_rw[3 5]
pc_rw6
r_adr[0 7]
adr_r8
adr_eq
sd[0 7]
sa[0 3]
rdata[0 7]
isp[0 2]
sdi_pc
sdo_pc
ior
iow
sysclk
PC-12V
PC+5V
VCC
GND
Scientific Systems Ltd
Unit 3 Howth Junction Bus Park,
Kilbarrack,
Dublin 5
Ireland
Title
PC Interface
Size B
Document Number
SSL PIM 10
Rev 3 0
Date Monday, September 18, 2000
Sheet 7 of 14

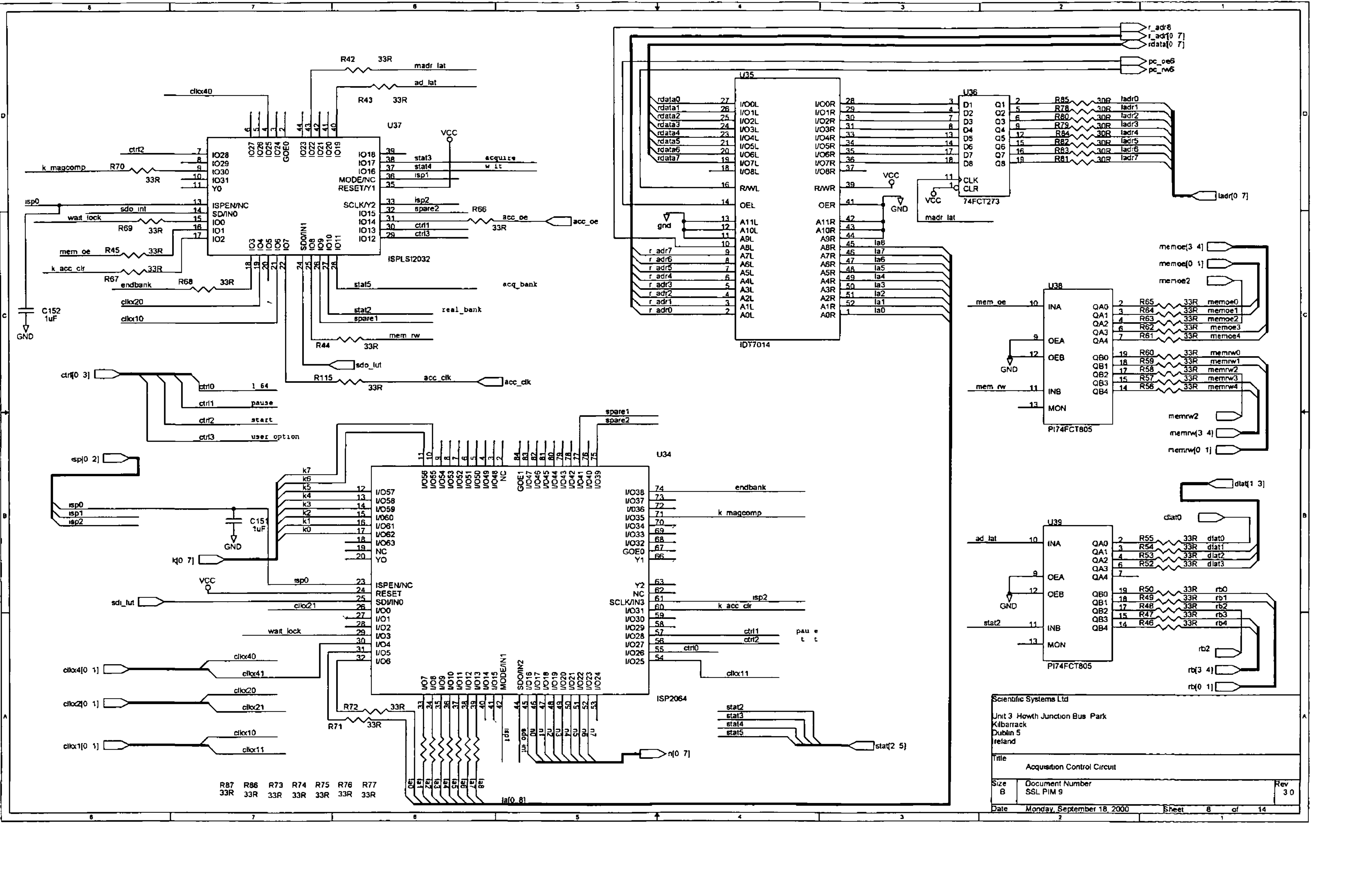
Scientific Systems Ltd
Unit 3 Howth Junction Bus Park
Kilbarrack
Dublin 5
Ireland
Title
Acquisition Control Circuit
Size
B
Document Number
SSL PIM 9
Rev
3 0
Date
Monday, September 18, 2000
Sheet 8 of 14

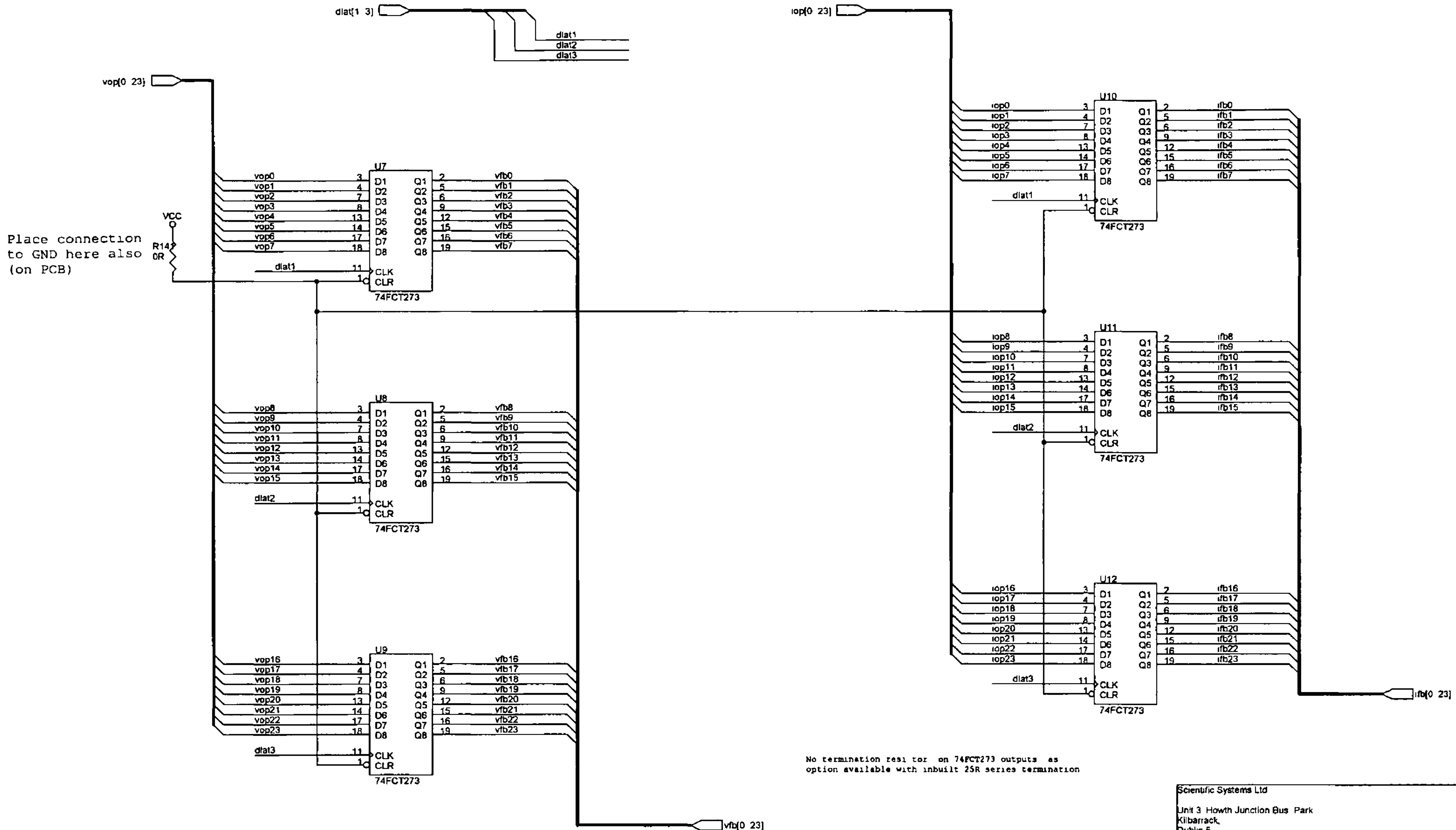

No termination resistor on 74FCT273 outputs as option available with inbuilt 25R series termination

Scientific Systems Ltd Unit 3 Howth Junction Bus Park Kilbarrack, Dublin 5 Ireland		
Title	Memory Data Feedback Latches	
Size B	Document Number SSL PIM 8	Rev 3 0
Date	Wednesday, May 05, 1999	Sheet 9 of 14

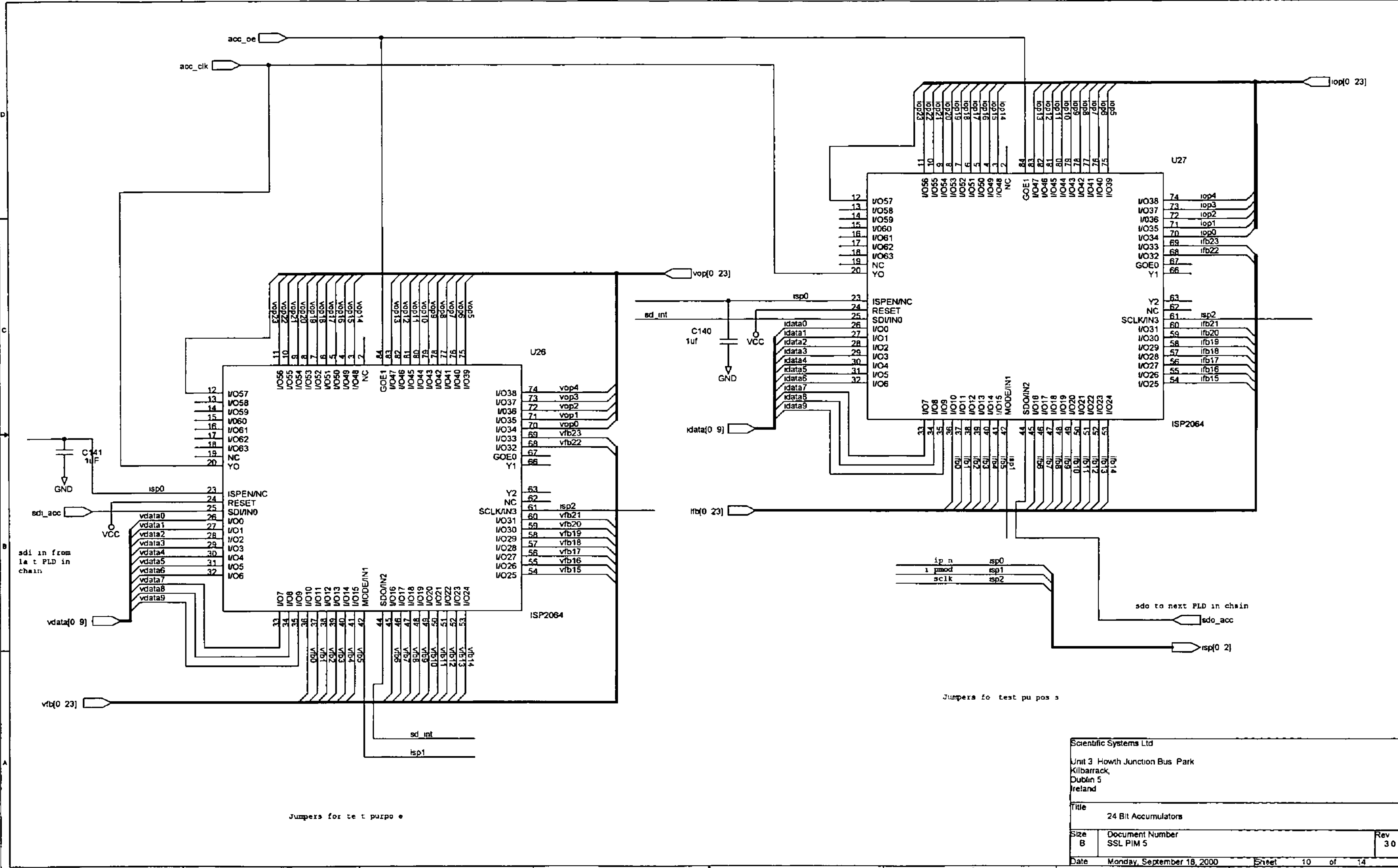
acc_oe
acc_clk
iop[0 23]
vop[0 23]
U26
U27
ISP2064
ISP2064
C141
1uF
GND
C140
1uf
GND
VCC
VCC
sdi_acc
sdi in from
la t PLD in
chain
vdata[0 9]
vfb[0 23]
idata[0 9]
ifb[0 23]
isp0
sd_int
isp1
sd_int
ip n
i pmod
sclk
isp0
isp1
isp2
sdo to next PLD in chain
sdo_acc
isp[0 2]
Jumpers for te t purpo e
Jumpers fo test pu pos s
Scientific Systems Ltd
Unit 3 Howth Junction Bus Park
Kilbarrack,
Dublin 5
Ireland
Title
24 Bit Accumulators
Size
B
Document Number
SSL PIM 5
Rev
3 0
Date
Monday, September 18, 2000
Sheet 10 of 14

Accumul tor Side of Memory

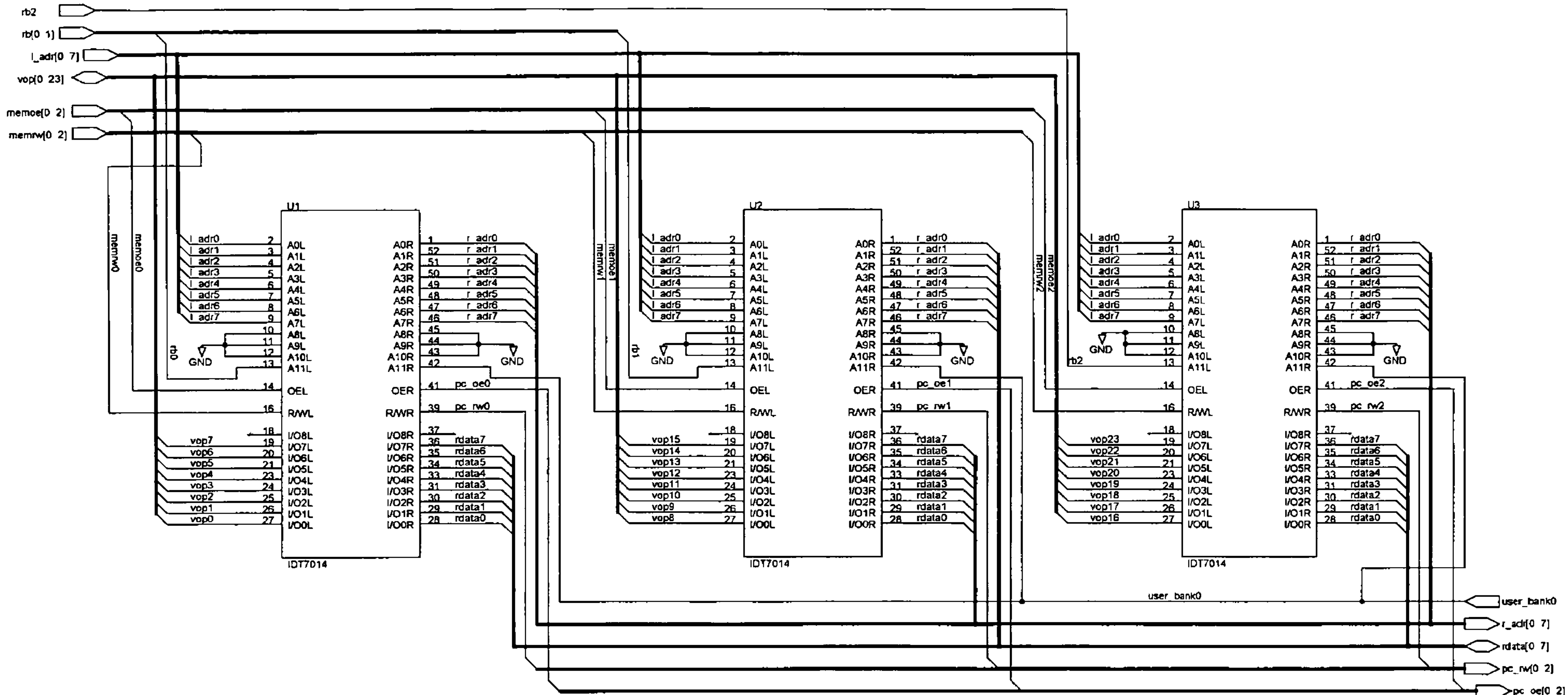

PC Sid of Memo y

Scientific Systems Ltd

Unit 3 Howth Junction Bus Park
Kilbarrack,
Dublin 5
Ireland

Title	Voltage Signal Dual Port Memory	
Size B	Document Number SSL PIM 6	Rev 3 0
Date	Monday, September 18, 2000	Sheet 11 of 14

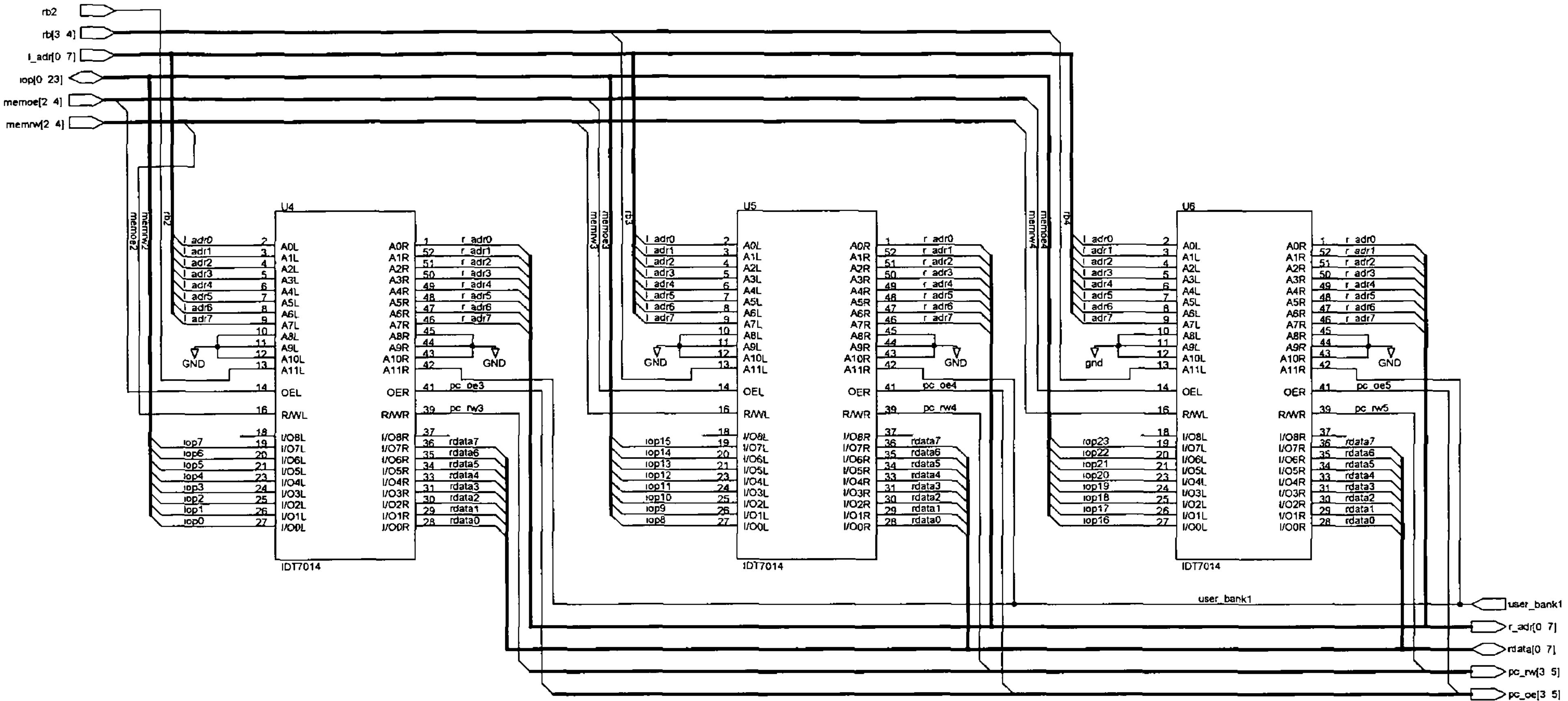

Scientific Systems Ltd		
Unit 3 Howth Junction Bus Park Kilbarrack Dublin 5 Ireland		
Title	Current Signal Dual Port Memory	
Size B	Document Number SSL PIM 7	Rev 3 0
Date	Monday, September 18, 2000	Sheet 12 of 14

External Trigger Optoisolators

U HCPL 0661 fo l w speed triggers
(Up to 10MBd)

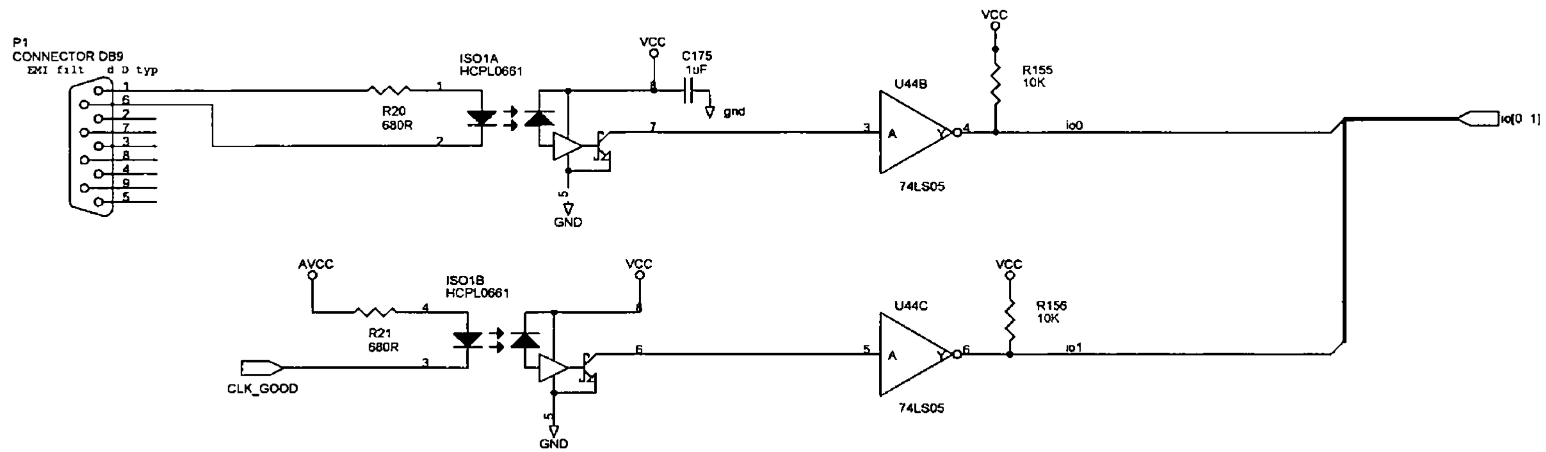

Scientific Systems Ltd Unit 3 Howth Junction Bus Park Kilbarrack, Dublin 5 Ireland		
Title: Digital Inputs		
Size: B	Document Number: SSL PIM 12	Rev: 3 0
Date: Monday, September 18, 2000	Sheet 13 of 14	

Analog Section Voltage Supply

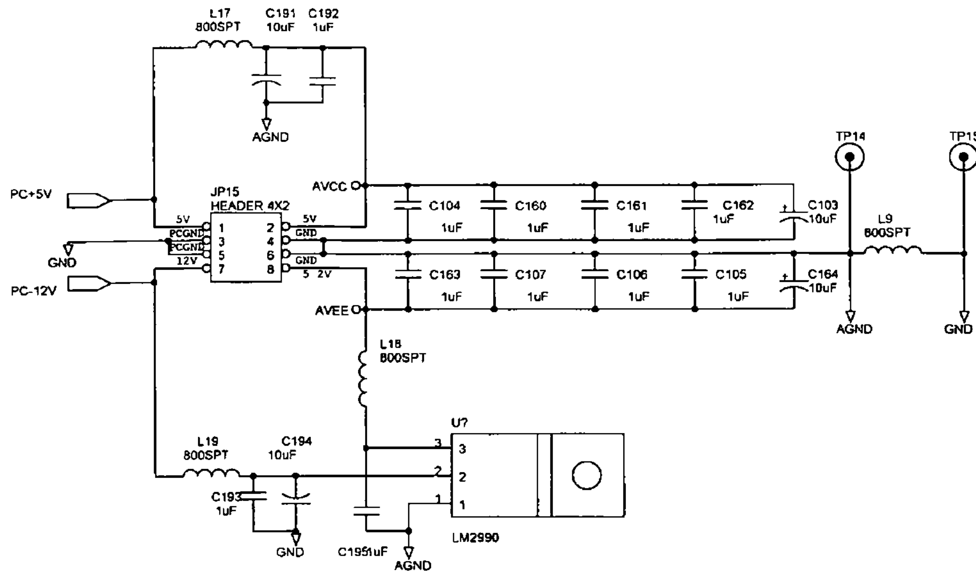

ISP Programming

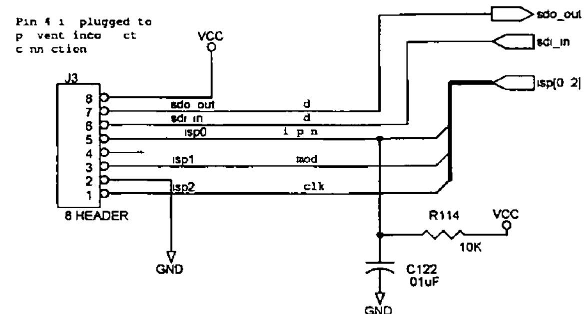

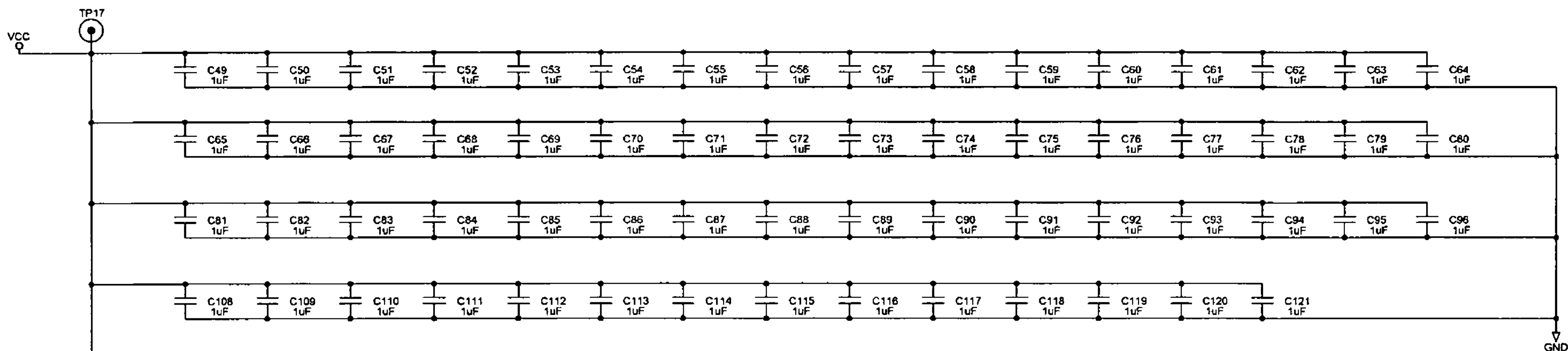

C97 10uF C100 10uF C98 10uF C99 10uF C101 10uF

GND

Decoupling and Storage Capacitors for Digital Sections

Pl minimum one 0 1uF capacitor pe pow r pin n h d vic nd
place one 10uF c p cito for each main logic sh t

Scientific Systems Ltd

Unit 3 Howth Junction Bus Park,
Kilbarrack,
Dublin 5
Ireland

Title: ISP and Decoupling

Size: B | Document Number: SSL PIM 13 | Rev: 3 0

Date: Monday, September 18, 2000 | Sheet 14 of 14

REFERENCES

1 Grill A, 1993 *Cold Plasma in Materials Fabrication* (IEEE Press)

2 Lieberman M A and Lichtenberg A J, 1994 *Principles of Plasma Discharges and Materials Processing* (Wiley)

3 Chapman B, 1980 *Glow Discharge Processes Sputtering and Plasma Etching* (Wiley)

4 Coonan B, 1996 Ph D Thesis (Dublin City University)

5 Scanlan J V, 1991 Ph D Thesis (Dublin City University)

6 Ibrahim Mahmoud Ahmed El-Fayoumi, 1996 Ph D Thesis (Flinders University of South Australia)

7 Li Y, Iizuka S and Sato N, 1996 *Plasma Sources Sci Technol* **5** 241

8 Oehrlein G S, Matsuo P J, Doemling M F, Rueger N R, Kastenmeier B E E, Schaepkens M, Standaert T and Beulens J J, 1996 *Plasma Sources Sci Technol* **5** 193

9 Keller J H, 1996 *Plasma Sources Sci Technol* **5** 166

10 Hopwood J, 1994 *Plasma Sources Sci Technol* **3** 460

11 Hopwood J, Guarnieri C R, Whitehair S J and Cuomo J J, 1993 *J Vac Sci Technol* A **11** 152

12 Hopwood J, 1993 *Appl Phys Lett* **62** 940

13 Ra Y, Bradley S G and Chen C-H, 1994 *J Vac Sci Technol* A **12(4)** 1328

14 Keller J H, Forster J C and Barnes M S, 1993 *J Vac Sci Technol* A **11(5)** 2487

15 Suzuki K, Nakamura K, Ohkubo H and Sugai H, 1998 *Plasma Sources Sci Technol* **7** 13

16 Hopwood J, 1992 *Plasma Sources Sci Technol* **1** 190

17 Gudmundsson J T and Lieberman M A, 1998 *Plasma Sources Sci Technol* **7** 1

18 Patrick R, Baldwin S and Williams N, 2000 *J Vac Sci Technol* A **18(2)** 405

19 Miller P A, 1991 *Proc SPIE Int Soc Opt Eng* **1594** 179

20 Hopwood J, Guarnieri C R, Whitehair S J and Cuomo J J, 1993 *J Vac Sci Technol* A **11(1)** 147

21 Colpo P, Ernst R and Rossi F, 1999 *J Appl Phys* **85(3)** 1366

22 Lloyd S, Shaw D M, Watanabe M and Collins G J, 1999 *Jpn J Appl Phys* **38** 4275

23 Miyazawa W, Tada S, Ito K, Saito H, Den S, Hayashi Y, Okamoto Y and Sakamoto Y, 1996 *Plasma Sources Sci Technol* **5** 265

24 Raoux S, Liu K S, Guo X and Silvetti D, 1998 *Mat Res Soc Symp Proc* **502** 53

25 Patrick R, Williams N, and Lee C G, 1997 *Proc SPIE Int Soc Opt Eng* **3213** 64

26 Lee S F and Spanos C J, 1995 *IEEE Trans Semiconduct Manufact* **8(3)** 252

27 Spanos C J, Guo H-F, Miller A and Levine-Parrill J, 1992 *IEEE Trans Semiconduct Manufact* **5(4)** 308

28 Godyak V A, Piejak R B and Alexandrovich B M, 1999 *J App Phys* **85(2)** 703

29 Almgren C, 1997 *Semiconductor International Magazine* **Aug** 99

30 Turner M M, 1993 *Phys Rev Lett* **71** 1844

31 Kim B and Lee C K, 2000 *J Vac Sci Technol* A **18(1)** 58

32 Miranda A J and Spanos C J, 1996 *J Vac Sci Technol* A **14(3)** 1888

33 Duffin W J, 1980 *Electricity and Magnetism* (McGraw-Hill)

34 Marion J B and Hornyak W F, 1982 *Physics for Science and Engineering* (CBS College Publishing)

35 Keane A R A, 1996 *US Patent 5,565,737*

36 Bentley J P, 1986 *Principles of Measurement Systems* (Longman Inc)

37 Defatta D J, Lucas J G and Hodgkiss W S, 1988 *Digital Signal Processing* (Wiley)

38 Data Translation Inc , Tutorial *ENOB (Effective Number of Bits) – The Accurate Way to Choose aData Acquisition Board*

39 Hopkins M, 1998 *US Patent 5,808,415*

40 Scientific Systems Ltd , 2000 *SmartPIM Application Note #3 – Match Unit Diagnostics*

41 Scientific Systems Ltd , 2000 *SmartPIM Application Note #4 – Etch End-Point*

42 Gerrish et al , 1998 *US Patent 5,770,922*

43 Turner et al , 1996 *US Patent 5,576,629*

44 Analog Devices, 1990 *High Speed Design Seminar Notes*

45 Koenig H R and Maissel L I, 1970 *IBM J Res Develop* **14** 168

46 van Roosmalen A J, van den Hoek W G M and Kalter H, 1985 *J Appl Phys* **58** 653

47 Bletzinger P, 1990 *J Appl Phys* **67** 130

48 Lieberman M A, 1988 *IEEE Trans Plasma Sci* **16** 138

49 Lieberman M A, 1989 *IEEE Trans Plasma Sci* **17** 338

50 Riemann K U, 1989 *J Appl Phys* **65** 999

51 Piejak R B, Godyak V A and Alexandovich B M, 1992 *Plasma Sources Sci Technol* **1** 179

52 Godyak V A, Piejak R B and Alexandovich B M, 1994 *Plasma Sources Sci Technol* **3** 169

53 Hopkins M, 2000 *US Patent 6,061,006*